Masters Theses   Student Theses and Dissertations

1968

Instrumentation of a shock tube facility

James Everett West

Recommended Citation

In dedication to my father

Mr. Harold E. West

INSTRUMENTATION OF A SHOCK TUBE FACILITY

BY

JAMES EVERETT WEST

A

THESIS

submitted to the faculty of the

UNIVERSITY OF MISSOURI - ROLLA

in partial fulfillment of the work required for the

Degree of

MASTER OF SCIENCE IN MECHANICAL ENGINEERING

Rolla, Missouri

1968

Approved by

Lyle G. Rhea (Advisor)   _R. B. Oetting_

R. Parker

ABSTRACT

The theory of schlieren and interferometer systems was described and related to studies of shock waves in a shock tube. An interferometer was procured and a schlieren system was modified for use with the UMR shock tube facility. The design and construction of a base for the systems and window assemblies for the shock tube comprised the major portion of the work on this project. A short series of tests were run to ascertain the compatibility of the instrumentation to the UMR shock tube facility.

While no schlieren photograph of the shock wave was obtained, the system was shown to be operating properly. The piezoelectric pressure transducers used in conjunction with a dual beam oscilloscope provided a record from which shock velocity and strength could be calculated. Test results were compared where possible to theoretical values and very good correlation was obtained.

1iii

ACKNOWLEDGEMENT

The author wishes to acknowledge the encouragement, advice and help given by his advisor, Dr. Lyle G. Rhea, during this course of study. The author also acknowledges the Space Science Research Center of the University of Missouri for its support of this project. The help and suggestions of Mr. Richard Smith, Mr. H. Sajon Joyner and Mr. Richard Riley were greatly appreciated. The author wishes also to thank Mr. Lee Anderson and his staff for their patience and suggestions during the construction of the equipment for this project. The moral support and encouragement from my wife and our parents was constantly appreciated.

TABLE OF CONTENTS

LIST OF FIGURES AND TABLES

LIST OF FIGURES AND TABLES (CONTINUED)

FIGURES

NOMENCLATURE

a	optical path designation
A_L	loaded area of plate
A_T	bolt tensile area
b	optical path designation
C	capacitance
c	velocity of sound
C_o	condenser (schlieren light source)
D_1 and D_2	diagonal mirrors
D_{max}	maximum bolt diameter
d	fringe separation
d_i and d_o	inner and outer diameters
E	charging voltage
F	force in bolt sets
f	frequency of light oscillation
g_c	gravitational constant
I	electric current
K_{G-D}	Gladstone-Dale constant
K_1, K_2 and K_3	knife-edge adjustments
k	spring constant
L	test section length
L_i	inductance
LS	light source

L_1	collimator (schlieren light source)
L_2	telescope lens (schlieren system)
M	mass
M_A, M_x and M_y	mach numbers
M_1 and M_2	parabolic concave mirrors
m	fringe order
N	an integer
n	refractive index
P	prism (schlieren light source)
p_o	unit loading of a flat plate
$p, p_x,$ and p_y	pressures
R and r	radius
R_g	gas constant
R_r	resistance
S_1 and S_2	light source slit
S_{max}	stress in plate
s	light path separation
T	absolute temperature
t	plate thickness
t_a, t_b	time
V, V_{vac}, V_m	light velocity
X, x, Y	cartesian coordinates
z	optical axis coordinate

cm	centimeters
ft.	feet, foot
Hg	Mercury
in.	inch
LBL	length bolt line
lbs.	pounds
mm	millimeter
mv	millivolt
no.	number
NB	number of bolts on bolt line
OPL	optical path length
OPLD	optical path length difference
pCb	picocoulomb
psi	pounds per square inch
psia	pounds per square inch absolute
psig	pounds per square inch gauge
sec.	second
sq.	square
UNF	Unified National Fine

π	constant $\cong 3.1416$
ρ	density
τ	time period
ζ	damping ratio
$\propto$	proportional to
$\partial/\partial n$	partial differential operator
ϵ	angle of light refraction
λ	light wavelength
λ_i	constant
δ	angular rotation
γ	specific heat ratio
μ	micro; 10^{-6}
σ_b	bolt stress
ω_n	natural frequency

I. INTRODUCTION

Shock tubes are becoming an ever more powerful tool for research

dealing with high temperature chemistry, physics and hypersonic aerodynamics.

Especially in areas dealing with aerodynamics and shock loading of structures,

flow visualization is very helpful. To provide the accurate visual records which

are so useful, optical methods are available to photograph the flow patterns.

Adapting an optical system for use with the shock tube requires windows on

the tube as well as the optical system and related equipment.

The University of Missouri at Rolla has a shock tube which was designed

and built in 1965 and was described by W. A. Crede (4). The shock tube has

three basic sections, the primary driver, secondary driver, and the test section.

Design pressures of each section are 10,000 psi, 5,000 psi, and 1,000 psi,

respectively. The primary driver is cylindrical in shape and a spring loaded

plunger is mounted internally in the section. The secondary driver is also

cylindrical, but with a slightly smaller internal diameter. The test section is

square with a total length of about twenty-one feet. The internal dimensions

of the test section are smaller than the dimensions of either driver section.

The method of operation of the tube is basically to separate the three

sections by clamping diaphragms, usually a metal sheet, between the primary

and secondary driver and between the secondary driver and the test section,

and then to suddenly release high pressure gas from the primary driver into

a chamber which is at a lower pressure. The separation allows a vacuum to

be drawn in the test section and some higher pressure to be built-up in the

driver sections. The diaphragm between the primary and secondary drivers is ruptured by releasing the plunger or simply by pressure breakage. A shock wave forms as the high pressure is released into the lower pressure and the shock wave, which is physically formed in the secondary driver, breaks the second diaphragm. It subsequently travels down the tube at a velocity which is dependent on the initial pressure ratios between the sections and the area changes. Operation of the tube in the single diaphragm mode can be accomplished by using only one diaphragm placed between the primary and secondary driver sections.

In preparing the facility for optical studies of the shock wave, provision must be made to permit light to pass through the sealed test section. The windows used must therefore seal the tube for both the vacuum and the high pressures associated with a shock wave. The window mounts must be able to withstand at least the same internal pressure as the test section itself.

To eliminate the possibility of scratching the windows, diaphragm material must be chosen such that diaphragm rupture does not shatter the material and hurl projectiles down the tube with the shock wave.

Two optical systems were considered for this facility. An interferometer was designed for use with a continuous beam helium-neon laser and a schlieren system was to use a single flash from a spark-gap or flash lamp. The continuous light from the laser was to be used with photodiodes to monitor fringe shift, but the spark-schlieren type photography required timing of the

single flash. The flash had to be timed to occur while the shock wave was in the usable portion of the light beam which passed through the tube perpendicular to the shock direction. Both optical systems were to be mounted on a single base, interchangably, and the base was to be mobile so that the systems could be used for steady state wind tunnel or shock tube studies.

Pressure transducers were to be used to monitor the static pressure in the tube. They were also to perform the functions of a light trigger for the schlieren system and a velocity determination base.

In this thesis are described the optical systems, an interferometer and a schlieren system, designed for and adapted to the University of Missouri at Rolla Shock Tube Facility. Also described are the mobile base used to support the optical systems, the window mounts and the shock tube modifications. The method of operating the schlieren system in connection with the two piezo-electric pressure transducers is detailed in an example test procedure.

II. LITERATURE REVIEW

Photographic studies of rapidly changing disturbances which create refractive index changes in a gas are usually accomplished by one of three methods: shadowgraph, schlieren or interferometer. Each of these systems required some optics, a light source and a photographic equipment.

The shadowgraph or direct shadow method proposed by Dvorak in 1880 is the simplest of the three methods. Basically the principle involves directing a point source of light toward a photographic plate. By flashing the high intensity light as a disturbance, such as a projectile, passes in front of the photographic plate, a shadow of the disturbance will be recorded on the plate. Shock waves also are observed by this method since the pressure change across the shock changes the index of refraction of the gas. The light ray deflection is proportional to the second derivative of density with respect to distance, $\frac{\partial^2 \rho}{\partial x^2}$.

The density gradient $(\frac{\partial \rho}{\partial x})$ is detected with a schlieren* system. The principle from which schlieren methods were derived was described by Foucault in 1859. He described a method for optically testing a mirror surface; now known as the Knife-edge test. The original suggestions of Foucault were developed by Toepler in 1864 for investigation of refractive index changes in liquids, flames, and pressure waves caused by spark discharges. Subsequently, his method has become known as the Toepler-Schlieren method

---

* German for striation. Striation is a form of striate; to mark with a fine streak or line, especially a number of parallel lines.

(Figure 1). Many experimental refinements have been incorporated in schlieren systems through the years. A common configuration now in use is the Twin-Mirror or "Z" system (Figure 13, Page 35). The use of concave mirrors in place of the very high optical quality schlieren head of the Toepler system lowers the cost and often shortens the overall length of the system. Taylor and Waldram proposed the two-pass system (Figure 2) to eliminate the observance of a double image from the concave mirror and at the same time doubled the sensitivity of their system because the light rays pass along the same path travelling both toward and away from the mirror.

The Mach-Zehnder interferometer (Figure 5, Page 19), which gives a direct method of measuring density, has been extensively in use as a tool in aerodynamic studies. The Twyman-Greene interferometer (Figure 8, Page 23) has been used for similar studies and in application to ionization produced by shock waves in shock tubes (11).

Spark-gaps have been used as light sources for high-speed photography for many years. G. A. Jones (10) describes some of the early methods of producing electric sparks showing both the gap configuration and firing circuits. To produce the intense light required to photograph high-speed airflow, a capacitor or bank of capacitors is usually discharged across an air gap. The method of initiating this discharge and controlling its position and duration are matters for continued development.

The amount of energy required to produce a sufficiently intense light depends on the characteristics of the circuit and upon the geometry of the gap
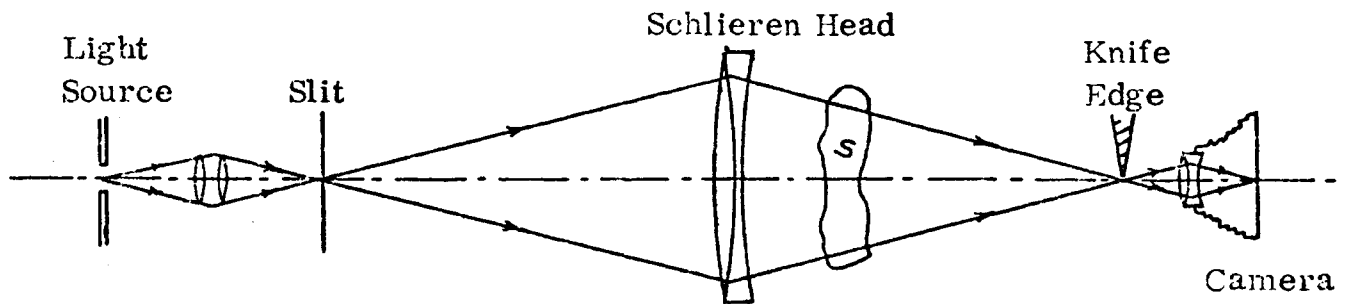
Light
Source   Slit   Schlieren Head   Knife
Edge

S

Camera

Figure 1.   Toepler Schlieren System

Light Source Slit
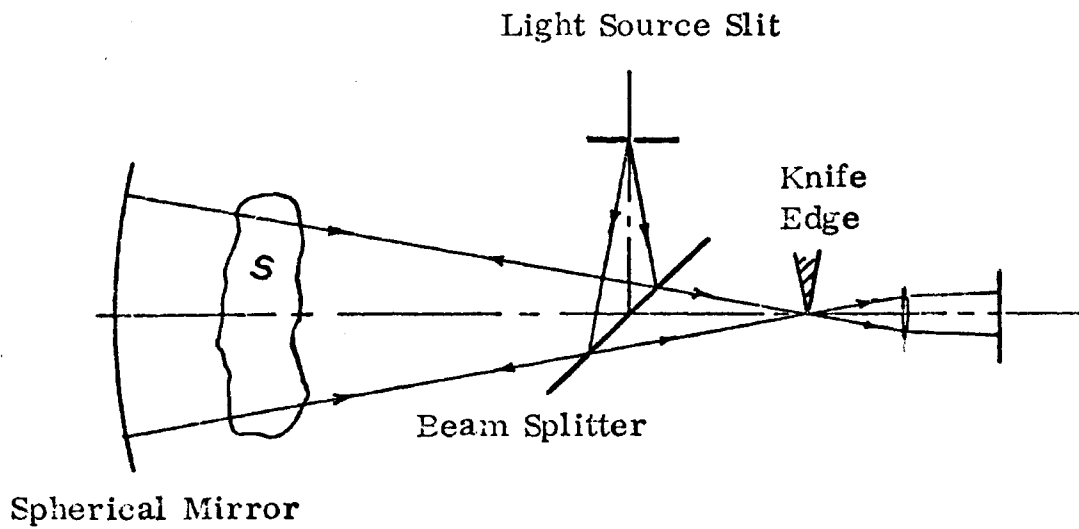
Knife
Edge

S

Beam Splitter

Spherical Mirror

Figure 2.   Taylor-Waldram Schlieren System

and optical system. The intensity problem is complicated by the fact that spark

duration times of 0.1 to 1.0 x 10^{-6} seconds are required for shock tube work.

Very short exposure times require more intense light, but increasing spark

intensity tends to increase the duration. Each application must, therefore, be

treated individually to effect a solution combining the maximum amount of

light produced in the shortest possible time.

Current in a discharge circuit depends on capacitance, C; inductance,

L_i; voltage, E; and other dissipative elements represented by a resistance, R_r.

The first peak of current in a lightly damped oscillatory discharge is given

approximately by

$$I = E(C/L_i)^{\frac{1}{2}}$$

with time period

$$\tau = 2\pi(CL_i)^{\frac{1}{2}}$$

and damping proportional to

$$\zeta \propto \exp(R_r/2L_i).$$

"A good capacitor, with both non-inductively assembled electrodes and short

internal connection is the prime requisite for a successful spark source."

(12).

Many spark-gaps used today are of the three electrode type described

in references 3, 6, 10, and 12. In this configuration a triggering circuit causes

a discharge to occur between a triggering electrode and one of the two main

electrodes causing instantaneous breakdown of the main gap. This discharge

is often constricted in a non-conducting cylinder to intensify the light and to make it as nearly a point source as possible. At times, a stream of inert gas is directed at the gap or the gap is sealed in an inert gas atmosphere to allow it to operate at higher voltages without undue electrode erosion or afterglow.

Gap geometry is a factor in focusing an optical system because the use of a hollow cylinder allows the spark to establish itself anywhere within the bore and it may change position from spark to spark. Also because of the geometry, "it is inadvisable to specify flashes from sparks by analogy with those from flash tubes, in terms of $\frac{1}{2}CE^2$; the luminous energy is not equal to this value and bears no constant relation with it."(12)

George A. Theophanis (21) described a "strip gap"which eliminated geometric instabilities of the arc and the third or triggering electrode. He found the arc stability to be good because of the short arc path and the third electrode to be unnecessary because the gap will break down under voltages at which cold cathode switch tubes operate.

One ingenious method for obtaining a spark of extremely short duration was described by J. W. Beams and his associates (2). They used a length of coaxial cable in place of the conventional capacitors. The circuit was so arranged that when the spark was triggered, a pulse traveled down the cable. As the pulse which was reflected from the end of the cable reached the gap, the potential at the spark-gap was reduced to zero. The spark duration was controlled by varying the length of cable used.

Using any of the three optical methods with a spark-gap light source to photograph high-speed airflow in a shock tube, the usual procedure is to take a series of pictures during a series of runs. If the flow pattern across an object is to be studied, each successive picture is delayed by a small amount from the preceding picture putting the flow at a different position on the body. This delay can be accomplished electronically by various circuits such as that described by E.K. Parks and R.E. Petersen. (14)

The flow in a shock tube is relatively reproducable for a series of pictures. However, small instabilities in the flow can cause a wide variation in the results from one run to the next. For this reason, H. Schardin (16) concluded that cinematography with a system having good space resolution and an adequate framing rate was particularly suited to identification of complicated phenomena.

Techniques for high-speed cinematography are numerous and are continually being improved. Many ultra-high-speed movie cameras are commercially available (8). Other techniques for providing the high framing rates necessary for shock tube cinematography use repetition flashing of a single gap or timed flashing of multiple sparks. Repetition flashing rates to 25,000 flashes per second have been achieved by F. Frungel (6) with his high-speed flash lamp. A multiple spark-gap system devised by C. Cranz and H. Schardin with repetition rates to one million per second for a few pictures is described in reference 2. The multiple spark-gap system at Cambridge University (7) is an application of the Cranz-Schardin system.

A. SCHLIEREN THEORY

Schlieren systems using lenses, mirrors or both are all basically the same. The schlieren system shows the gradient in index of refraction since light passing through a density gradient in a gas is deflected in the same manner as though it were passing through a prism. The index of refraction of a gas is dependent upon the density, the speed of a wavefront of light varies inversely with the index of refraction, n, of the medium. Thus, a given wavefront will rotate as it passes through a gradient in density which represents also a gradient in refractive index.

While the physical components of schlieren systems vary, the basic system set-ups are similar. A light source is usually focused at a slit or knife-edge in order to produce a point or line source of light. This light can be handled in many ways. It can be focused again by a large, highly corrected lens (Figure 1) or collimated by a lens and then focused by a second lens. It can be focused by a concave mirror or collimated by a concave mirror (Figure 13, Page 35) and then focused by a second mirror. The test section is positioned in the collimated section of the beam or in the focusing portion of the beam in the respective systems. At the point of refocus of the beam, a knife-edge is placed exactly parallel to the slit source. By careful adjustment, a very narrow effective path is created for the light.

As the second knife-edge is slowly moved across the focal point, the observed phenomenon with no disturbance present in the system is that a uniformly illuminated field is observed until the knife-edge has entirely

crossed the focal point. Then the entire field becomes dark.

To examine qualitatively the schlieren principle, assume that the knife-edge just blocks all the light. If now a disturbance of refractive index occurs in the test section, light rays will be deflected toward or away from the knife-edge. Those rays deflected toward the knife-edge will not pass the stop while those deflected in the opposite direction will pass over the knife-edge and can be observed. Some light rays may also be deflected parallel to the knife-edge. These rays will not produce any change in the observed image.

Common practice in preparing the system for a test is to adjust the knife-edge to allow approximately half the light to pass the focal point thus providing a low illumination background for study of the striations.

For each elemental volume in the test section which produces a deviation in light direction not parallel to the knife-edge, a point on the viewing screen will be more or less intensely illuminated and the composite of all these points forms the image of the phenomenon being investigated. The presence of the background allows the outline of the disturbance to be seen more easily.

Since only those deflections which are not parallel to the knife-edge become visible, aligning the knife-edge and slit parallel to an "X" axis makes visible the density gradients in the "Y" direction. By rotation, the axes can be changed to any position, always making visible those gradients of density perpendicular to the particular orientation of the knife-edge. By rotating the knife-edge and slit through successive steps for successive pictures a complete picture of the flow pattern can be obtained; providing the flow pattern does not

change or that it can be reproduced.

Refractive index of a medium is defined as

$$n = \frac{V_{vac}}{V_m} \tag{1}$$

where V_{vac} is the light velocity in a vacuum and V_m is the light velocity in the medium. Thus the velocity of a given wavefront of light varies inversely with the index of refraction,

$$V_m = \frac{V_{vac}}{n} \tag{2}$$

and the wavefront will rotate as it passes through a gradient in n. The wavefront rotation causes the normal to the wavefront to follow a curved path (Figure 3); since the normal is really the light ray, the latter is refracted as it passes through the density gradient. Noting that n is nearly unity for gases, it may be shown (App. III) that

$$\frac{1}{R} = \text{gradient n} \tag{3}$$
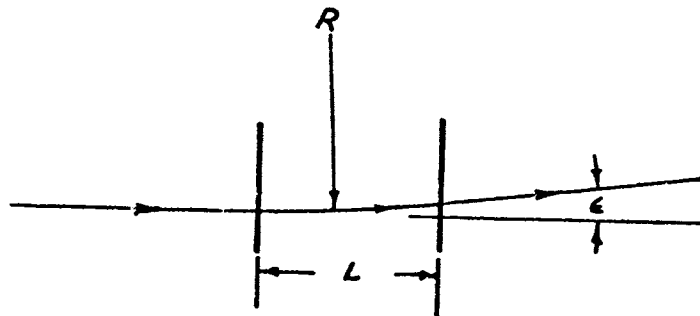
where R is the radius of curvature of the light ray.

Figure 3. Wavefront Rotation

The Gladstone-Dale equation

$$\frac{n-1}{\rho} = K_{G-D} \tag{4}$$

is used to relate the index of refraction to the gas density. In the equation, n represents the index of refraction; ρ is the density; and K_{G-D} is the Gladstone Dale constant. K_{G-D} is an experimentally determined constant which occurs as a case of the theoretical law known as the Lorentz-Lorentz law. This special case, for a gas at constant temperature, indicates that the value (n-1) is directly proportional to the pressure and thus the density.

$$\frac{n^2 - 1}{n^2 + 2} = (n - 1)\frac{n + 1}{n^2 + 2} = \text{const} \times \rho \tag{5}$$

When n is very nearly unity, as is the case with gases, the factor $(n + 1)/(n^2 + 2)$ is nearly constant as required by equation 5.

Now to examine two adjacent paths, a and b, which are separated by a distance Δs, use equation 4 to write to the index of refraction of both paths as,

$$n_a = K_{G-D}\,\rho_a + 1$$

$$n_b = K_{G-D}\,\rho_b + 1 \; . \tag{6}$$

Subtracting and dividing by Δs

$$\frac{n_a - n_b}{\Delta s} = \frac{K_{G-D}\rho_a + 1 - K_{G-D}\rho_b - 1}{\Delta s} \tag{7}$$

$$\frac{n_a - n_b}{\Delta s} = \frac{K_{G-D}(\rho_a - \rho_b)}{\Delta s}$$

$$\lim_{\Delta s \to 0} \frac{\Delta n}{\Delta s} = K_{G-D} \lim_{\Delta s \to 0} \frac{\Delta \rho}{\Delta s}$$

$$\frac{\partial n}{\partial s} = K_{G-D} \frac{\partial \rho}{\partial s} \tag{8}$$

Keeping in mind that only those gradients not parallel to the knife-edge become visible, the coordinates X or Y can be substituted for s as the situation demands. Thus for density gradients in the X direction with the knife-edge aligned perpendicular to it,

$$\epsilon_x = \frac{L}{R} = L(GRAD\ n) = L\frac{\partial n}{\partial x} = L K_{G-D} \frac{\partial \rho}{\partial x} \tag{9}$$

While these relationships are fairly simple, strict quantitative evaluations from schlieren pictures are quite tedious and involve precise measuring of relative intensities on a photograph along with ray tracing through the geometry of the optical system. For these reasons, and others described by H. Schardin (16), qualitative interpretation of schlieren pictures is the most common practice. Qualitative study yields much information about a flow field and is quite adequate in many cases.

In application to shock tubes and wind tunnels, qualitative examination of a series of schlieren pictures is commonly used to study the flow field near a projectile or aerodynamic surface in simulated supersonic flight.

If more detailed information is needed about the densities, the Mach-Zehnder interferometer is a standard instrument used for quantitative examination of flow fields. However, by making use of Fraunhofer diffraction (Figure 4), a schlieren system can be used to obtain the same type of results which previously required the use of the interferometer.

B. SCHLIEREN INTERFEROMETRY

E. B. Temple (20) described the modifications which allow a schlieren system to yield quantitative results by interference fringes. The principle of this modification is that a plane wavefront in a collimated beam of light is distorted in its passage through a region of variable density, and as a result a variable phase distribution is produced in an exit plane which lies just beyond the disturbance and is perpendicular to the direction of propagation of the collimated beam (optical path). The tremendous rapidity of optical oscillations normally makes this phase distribution invisible, but it can be converted to an intensity distribution in which the maxima and minima of intensity correspond to points in the exit plane where the optical path length differs from that in an undisturbed portion of the plane by an integral number of half wavelengths. This can be done in a conventional schlieren system by reducing the light source slit to about 0.05 mm width and forming an image of the exit (object) plane with a convex lens or concave mirror. A small absorbing object or other appropriate modification is then inserted in such a way as to block the central maximum of the Fraunhofer pattern due to the free field (Figure 4).

Very little disturbance light is cut off in the process since this light is refracted and does not go through the focal point. The blocking of the free-field light sets up a diffraction process which causes this light to spread into the bordering disturbance image. The resulting interference produces the intensity band system.

Intensity Distribution of
the image of a small light
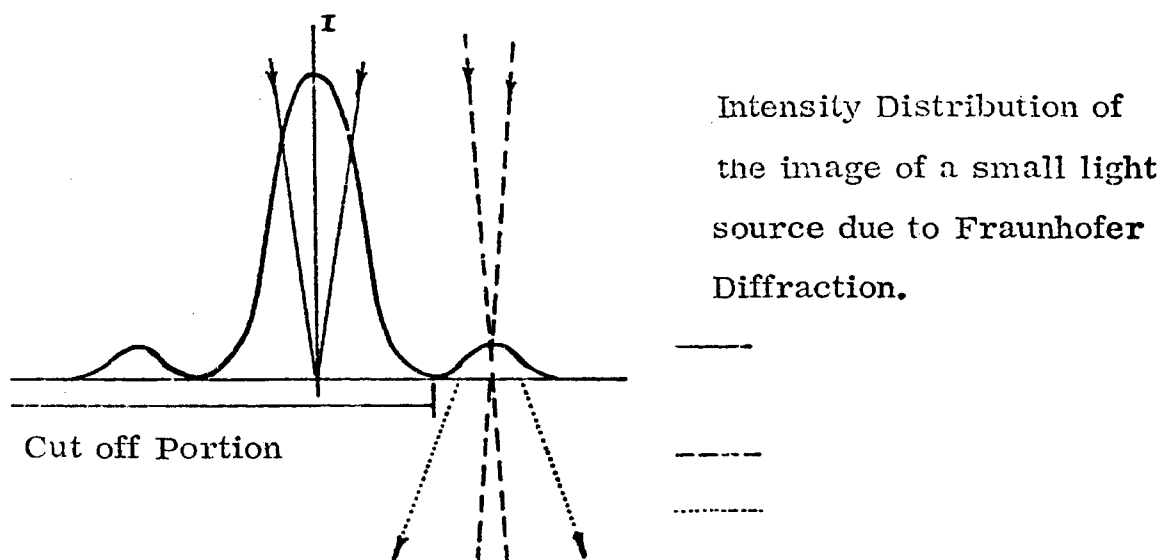source due to Fraunhofer
Diffraction.

Cut off Portion

Figure 4. Fraunhofer Diffraction Pattern

If the disturbance is two-dimensional, with density gradient vectors perpendicular to the optical axis, the measurement of the phase distribution is equivalent to a measurement of density by virtue of the Gladstone-Dale equation (equation 4).

Assuming that a monochromatic line source of wavelength λ is collimated before passing through the test section, the test section would be uniformly illuminated if there were no disturbance throughout the optical system. As a pressure change disturbs the test section, the density and thus the refractive index changes. The interference fringes formed according to the Fraunhofer Diffraction principle are practically a picture of iso-optical path length. At the lines of maximum light intensity the optical path length is found for each path by

$$\int_O^L n\, dz = OPL$$

where L is the length of the test section, n is the index of refraction, dz is

the differential length of the optical axis z, and OPL is the optical path length.

The optical path length difference, OPLD, between two bright fringes is $N\lambda$, where $N = 0, 1, 2, \cdots$ denoting the fringe order. At a point of minimum light intensity, OPLD equals $(N + \frac{1}{2})\lambda$ from a given bright fringe.

With flow containing density gradients, a fringe pattern is formed such that

$$\int_O^L n \, dz = \int_O^L (1 + K_{G-D}\rho) \, dz \tag{10}$$

is a constant on any one fringe, bright or dark, and changes by λ for adjacent bright or dark fringes. That is to say the optical path to one bright fringe is λ longer than the OPL to the adjacent bright fringe. Thus for two-dimensional flow, $\rho = \rho(x, y)$ where $(1 + K_{G-D}\rho)L$ is constant along any one fringe, knowing ρ along any one fringe allows ρ of all other fringes in the field to be calculated by

$$(1 + K_{G-D}\rho_2)L = (1 + K_{G-D}\rho_1)L + N\lambda. \tag{11}$$

N is again an integer which denotes the fringe order, L is the physical length of the test section, ρ_1 is a known density of one fringe and ρ_2 is the density of the fringe to be calculated.

Some physical knowledge of the way in which the density changes in the field is desirable so that any fringe could be chosen as the reference fringe.

C. INTERFEROMETRY

The Mach-Zehnder interferometer (Figure 5) is an instrument commonly used for density measurements in high-speed gas flows in shock tubes and wind tunnels. The interferometer consists of a point light source with collimating optics followed by a beam splitter (plate) to allow the light to travel over two separate paths before being recombined. The paths are of equal optical lengths and one path passes through the test section while the other does not pass through any medium which would disturb it. If all mirrors and beam splitters are exactly parallel and the path lengths are equal (plus or minus a few wavelengths), the image observed after recombination of the rays is a uniformly illuminated field with interference fringes focused theoretically at infinity. By changing one path length by one half wavelength, $\lambda/2$, the field would appear uniformly dark. All optical components of the system must be optically perfect and are normally flat and parallel to 1/10th wavelength to assure good results.

The interference fringe pattern which is quite often the most easily observed is that of localized fringes. These fringes which are nearly straight lines can be produced by rotating one plate, such as at the point of recombination of the rays in figure 5, through a small angle δ. These localized fringes are also called fringes of equal width because they effectively indicate the path difference included in a wedge with a wedge angle δ.

In Figure 6, the beams A and B would combine at the plate surface and follow the path that A takes to the screen if all plates and mirrors were exactly parallel. When the plate is rotated through the angle δ, the beam A
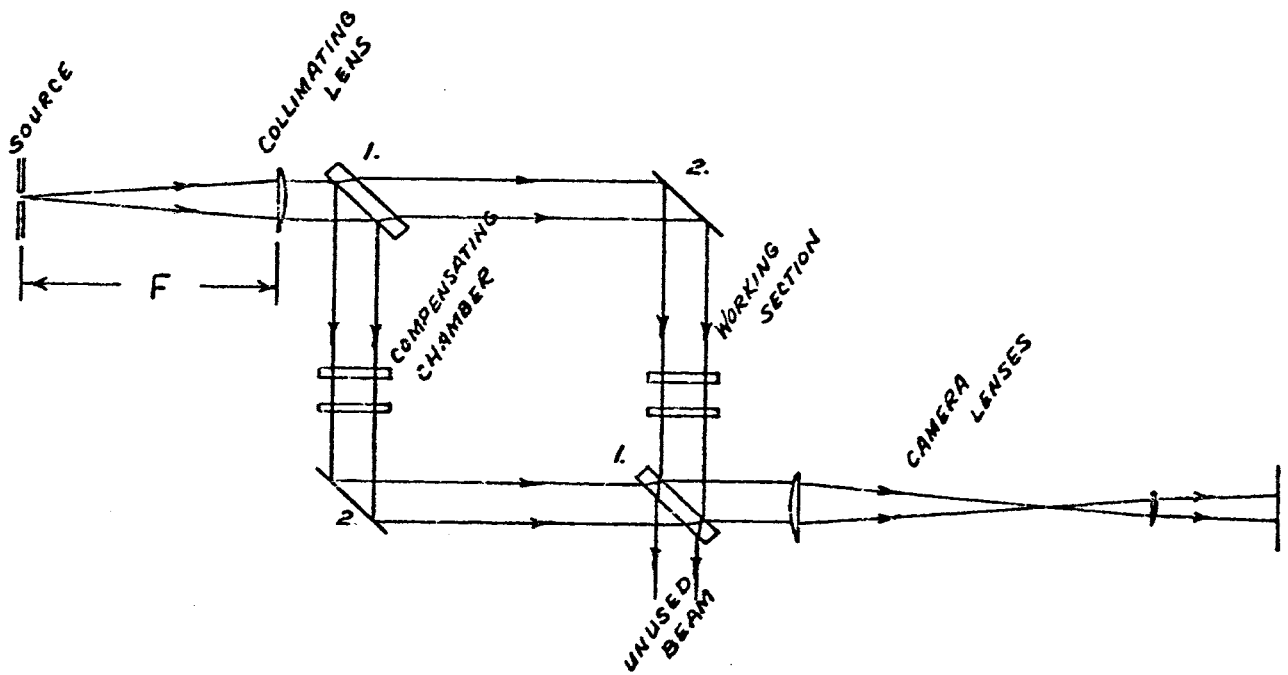
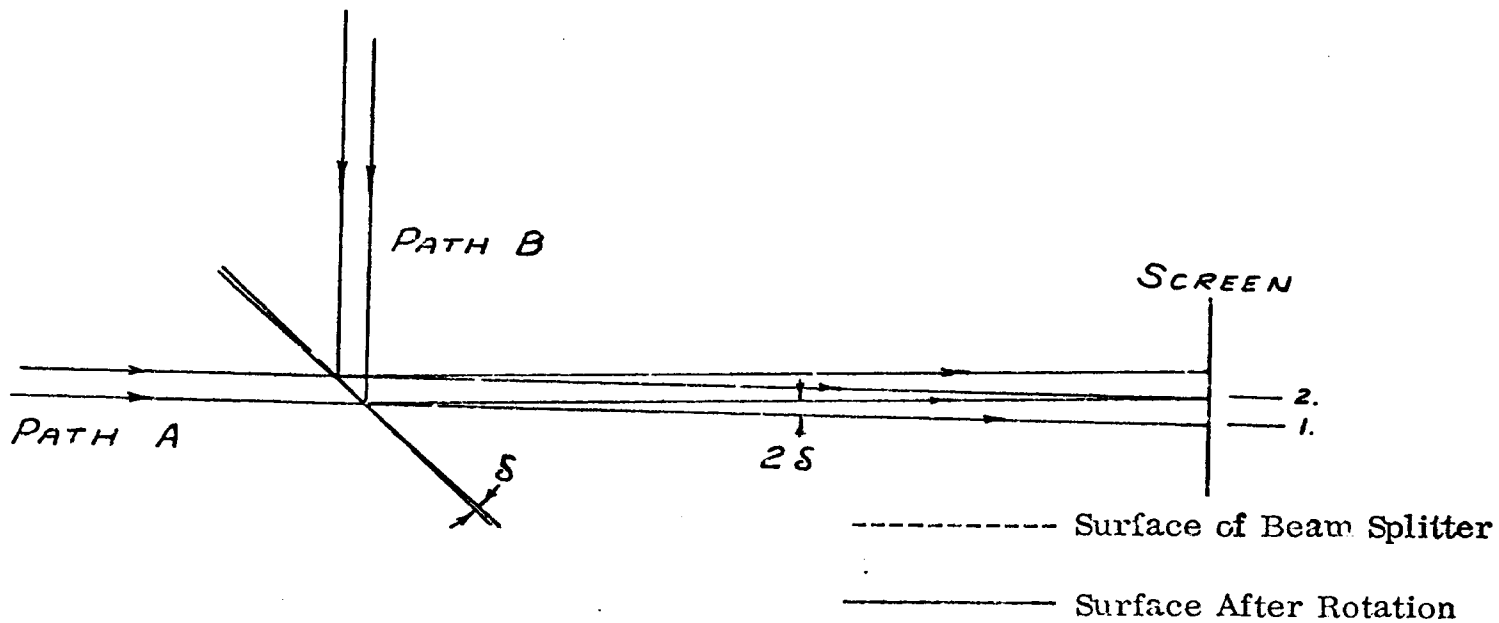Figure 5.   General Arrangement of Mach-Zehnder Interferometer

Figure 6. Localized Fringe Formation

is unaffected, but B is reflected along a path which is at an angle 2δ from the
path of A.

Assume that at point 1 the optical paths of all rays arriving at the point
are such that constructive interference occurs. At some point 2, at a distance
d from point 1 (Figure 7), constructive interference again occurs as one path is
now one wavelength, λ, longer than the other path arriving at the point. At a
point midway between 1. and 2., destructive interference occurs resulting in
a dark fringe where the path lengths differ by λ/2. These fringes are actually
lines which would be perpendicular to the page in Figures 6 and 7.

For all angles less than six degrees, the trigonometric functions of sine
and tangent are approximately equal to the angle expressed in radians. Then,
since δ is much less than one degree for this application

$$\tan 2\delta = \sin 2\delta = 2\delta$$

Also because δ is small, the separation of the bright fringes, d, (Figure 7) is approximately the hypotenuse of a right triangle, making

$$\sin 2\delta = \frac{\lambda}{d}$$

or

$$d = \frac{\lambda}{2\delta} \tag{12}$$

and more generally

$$Nd = \frac{N\lambda}{2\delta}$$
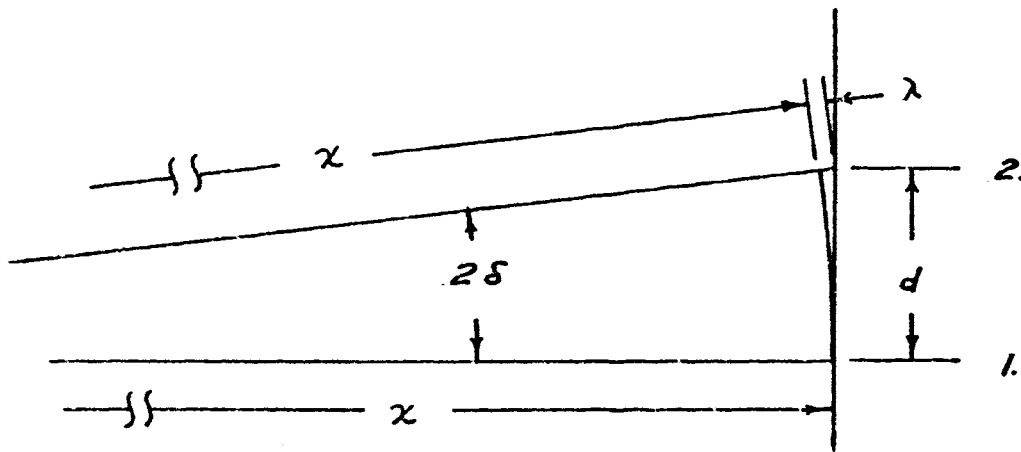
where N is the integral number of wavelengths.

Figure 7. Localized Fringe Formation (Enlarged)

The fringe separation and width can thus be controlled by the magnitude of the angle δ.

With the Mach-Zehnder interferometer, a slight rotation of the plates in opposite directions produces the angle δ and allows the fringes to appear to be localized at any convenient position along the optical paths. Localizing the fringes within the test section allows a photograph to be taken with the fringes and the object being studied in focus at the same time.

With the Twyman-Greene interferometer (Figure 8) the angle δ is usually controlled by rotation of one of the mirrors through the desired angle.

Assume now that all adjustments have been made to produce a system of localized fringes. By increasing the pressure of the gas in the test section, a continuous change in index of refraction is created. With the refractive index change, a change in optical path length occurs causing the observed fringes to move across the field. This optical path length change is

$$(n_f - n_i) L = \Delta OPL \tag{13}$$

where i and f represent initial and final states, respectively, and L is the test section length. This change produces a fringe shift of order m such that

$$(n_f - n_i)L = m\lambda \tag{14}$$

The order m represents the number of bright (or dark) fringes observed to move past a fixed point. The order of fringe shift for localized fringes may also be determined by measuring the distance a given dark fringe moves, 1, and dividing this value by the fringe separation, d

$$m = 1/d \tag{15}$$

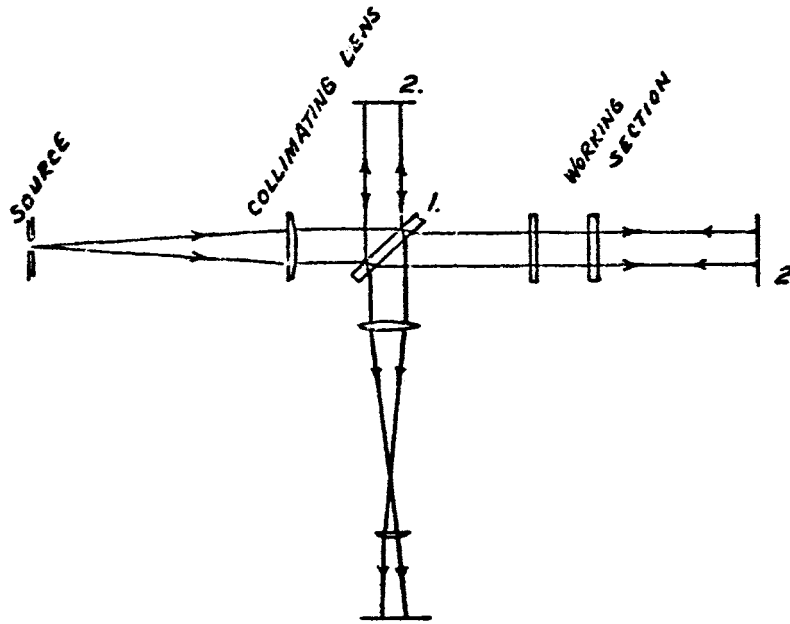To examine two samples of gas, a and b, which are at slightly different

Figure 8.   General Arrangement of Twyman-Greene Interferometer

pressures but of precisely the same physical length, L, each sample is placed

in a beam of monochromatic light emanating from a single point source. Let

the optical paths be such that the time difference for the light to traverse the

distance through a and b is

$$t_b - t_a = \frac{m\lambda_{room}}{V_{room}}$$ (16)

where t is the time, V is the light velocity, and m is the number of light cycles

difference in the paths. The value of m can change as the time difference changes

and indicates the fringe order or fringe shift. To relate the physical length,

L, of the test section to the time difference of the two paths

$$t_b - t_a = \frac{L}{V_b} - \frac{L}{V_a}$$ (17)

The index of refraction, equation one, allows the light velocities in a and b to

be written as

$$V_a = \frac{V_{vac}}{n_a} \qquad \text{and} \qquad V_b = \frac{V_{vac}}{n_b}$$ (18)

Then

$$t_b - t_a = \frac{L}{V_{vac}/n_b} - \frac{L}{V_{vac}/n_a} = \frac{L}{V_{vac}} (n_b - n_a)$$ (19)

From the original definition of $(t_b - t_a)$, equation 16,

$$\frac{L}{V_{vac}} (n_b - n_a) = \frac{m\lambda_{room}}{V_{room}}$$ (20)

The frequency of oscillation

$$f = \frac{V}{\lambda}$$ (21)

is a constant for monochromatic light. Thus

$$\frac{\lambda_{room}}{V_{room}} = \frac{1}{f} = \frac{\lambda_{vac}}{V_{vac}} \tag{22}$$

and

$$n_b - n_a = \frac{m\lambda_{room}}{V_{room}} \frac{V_{vac}}{L} = \frac{m}{f} \frac{V_{vac}}{L}$$

$$n_b - n_a = \frac{mV_{vac}}{L V_{vac}/\lambda_{vac}} = \frac{m\lambda_{vac}}{L} \tag{23}$$

which is equivalent to equation 14.

If sample "a" is chosen as a reference state and the value of n_b

changes, a fringe shift of order m could be observed, where m again represents

the number of light cycles difference in the paths.

Again in order to relate the index of refraction and the gas density,

the Gladstone-Dale equation (Equation 6) is used. The refractive index for

paths a and b are

$$n_a = K_{G-D} \rho_a + 1 \quad \text{and} \quad n_b = K_{G-D} \rho_b + 1 \tag{24}$$

Subtracting,

$$n_b - n_a = K_{G-D} \rho_b + 1 - K_{G-D} \rho_a - 1$$

$$n_b - n_a = K_{G-D}(\rho_b - \rho_a) \tag{25}$$

Equating 24 and 23

$$K_{G-D}(\rho_b - \rho_a) = \frac{m\lambda_{vac}}{L} \tag{26}$$

which is usually written

$$\rho_b - \rho_a = \frac{m\lambda_{vac}}{L\,K_{G-D}} \qquad (26)$$

With localized fringes, the fringe shift m can be expressed as

$$m = \frac{1}{d} \qquad (15)$$

and an alternate form of equation 26 becomes

$$\rho_b - \rho_a = \frac{\lambda_{vac}}{L\,K_{G-D}}\,\frac{1}{d} \qquad (27)$$

In equations 26 and 27, the densities of the gas samples have been related

to the wavelength, λ , of a known monochromatic light, the physical length of

the sample or test section, L and the Gladstone-Dale constant, K_{G-D}.

Determination of the fringe shift, m, is then necessary to complete the

calculation of the difference in the two densities. If the density of one sample

of gas is known, the other density can be calculated from equations 26 and 27.

III. EXPERIMENTAL EQUIPMENT

In planning further instrumentation for the University of Missouri at Rolla Shock Tube Facility (4), it was felt that a schlieren system to photograph the shock wave would be the most versatile optical system available. In connection with another specific project, however, a Twyman-Greene interferometer was the most suitable instrument. The Twyman-Greene interferometer would also double as a two-pass schlieren system for shock tube and wind tunnel use by covering one mirror. Therefore an interferometer was designed to serve these two purposes employing a laser as a light source. The laser selected was a continuous beam helium-neon type with light output of 6328 angstrom wavelength. Since it was a continous source, a high-speed movie camera was needed to take schlieren pictures. Because no camera was available with adequate framing rate (greater than 25,000 pictures per second) the decision was made to modify an existing schlieren system (1) to employ a flash lamp light source in order to achieve the short exposure time necessary for good photographs. The pressure transducers which were used for velocity measurements were thus used also to trigger the light source firing circuit.

The interferometer (Figure 9) will consist of two plane mirrors placed at right angles to each other and on opposite sides of the shock tube. A beam splitter plate will divide the collimated laser beam and direct the two parts at the mirrors. One of the beams will necessarily pass through the shock tube. After reflection, the beams will be rejoined at the beam splitter and the resulting interference pattern may be detected, displayed or photographed as desired.
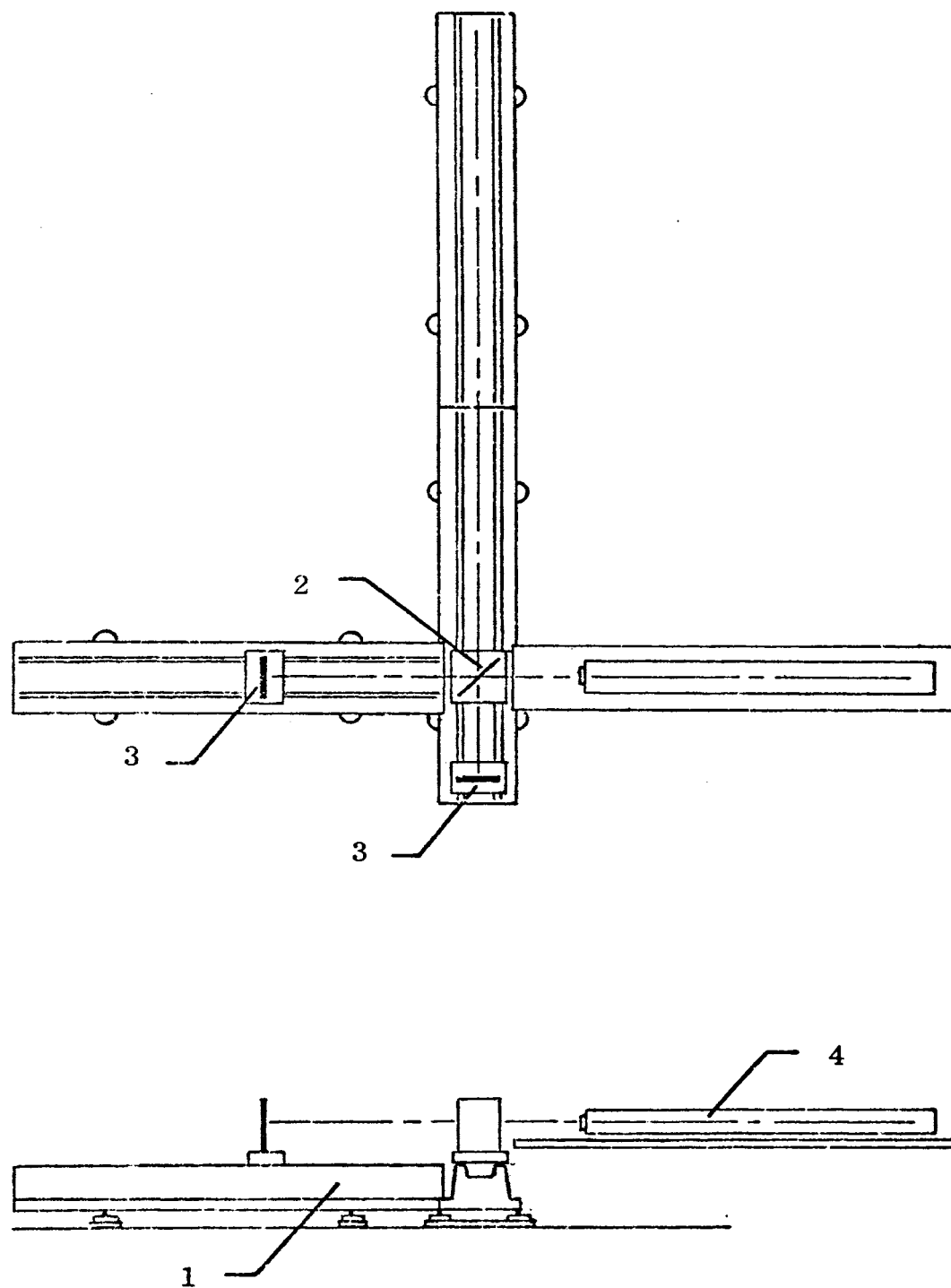
1. Optical Benches   3. Plane Mirrors

2. Beam Splitter   4. Laser

Figure 9.   Interferometer for UMR Shock Tube Facility

All optical components of the system are to be mounted on lathe-bed type optical benches to make aligning and focusing the system as easy as possible. The optical benches will be mounted on the specially designed and constructed mobile base.

Design requirements for the mobile base (Figure 10) were: 1) that it be heavily constructed to provide a solid base for the interferometer, and 2) that it be easily movable for use with either the shock tube or wind tunnel. Limitations on the height and geometry of the base were imposed by the height of the shock tube and by the supports on which the tube rested.

Since optical systems are very sensitive to vibrations, especially high frequency vibrations, the base for the systems should be rigid to prevent relative motion of the components and yet a low natural frequency ($\omega_n = \sqrt{k/m}$) is desirable to reduce the effect of transmitted vibrations. The spring constant, k, for the base was kept fairly low by mounting the entire system on low pressure pneumatic tires. System mass, M, and rigidity were provided by the use of an 8" x 8" wide flange H-beam (about 34 pounds per foot) as the basic structural component.

The laser beam to be used for interferometry will be about 2 mm in diameter, which means that vertical motion of the beam will be required to enable the user to investigate a composite cross-section of the shock wave. Windows for the interferometer are about three-eighths inch in diameter and will be mounted off-center in their window disks (Figure 11) which can be rotated. This rotation will move the window laterally as well as providing the vertical motion required. Thus the interferometer will be required to
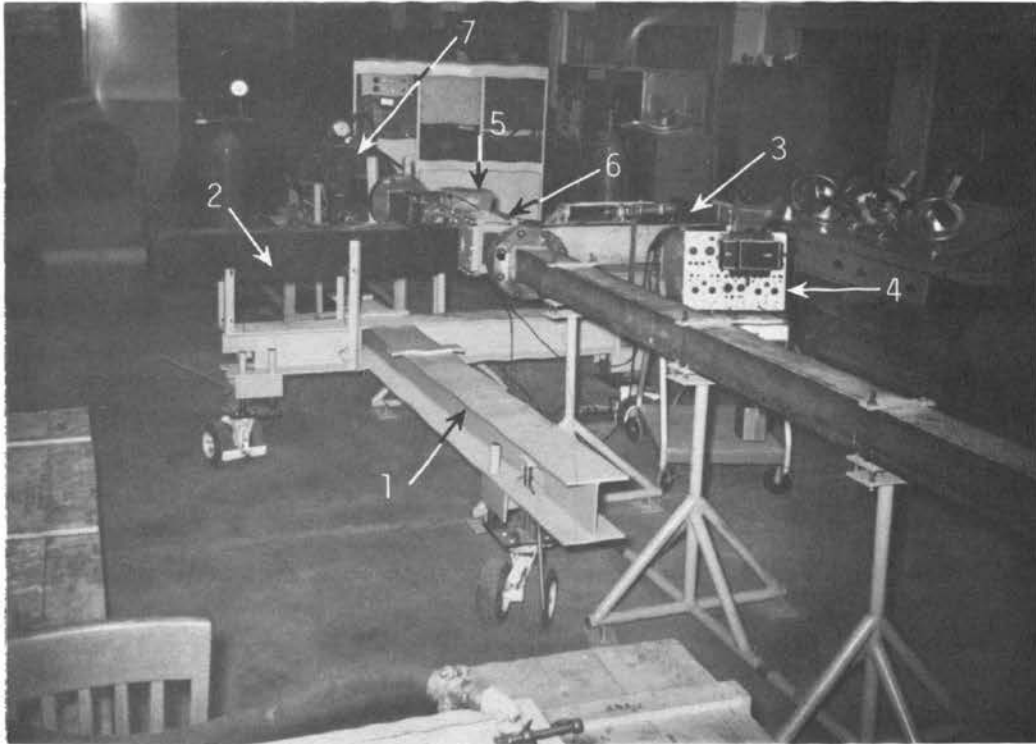
1. Mobile Base
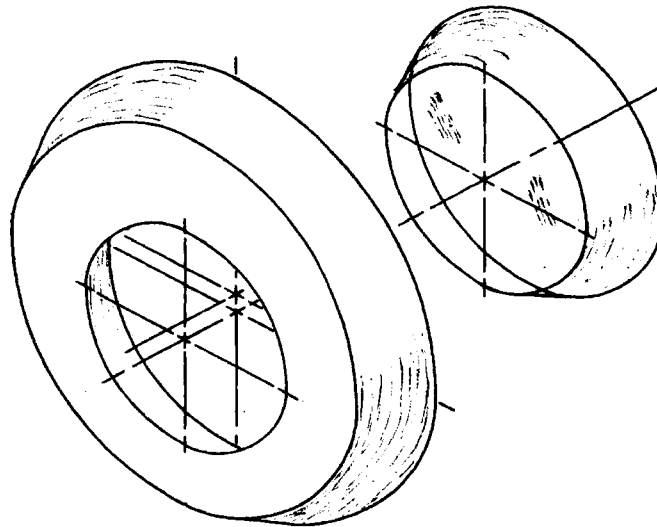2. Schlieren System
3. Schlieren Light Source
4. Oscilloscope
5. Charge Amplifiers
6. Test Section
7. Driver Sections

Figure 10.   Experimental Equipment Setup
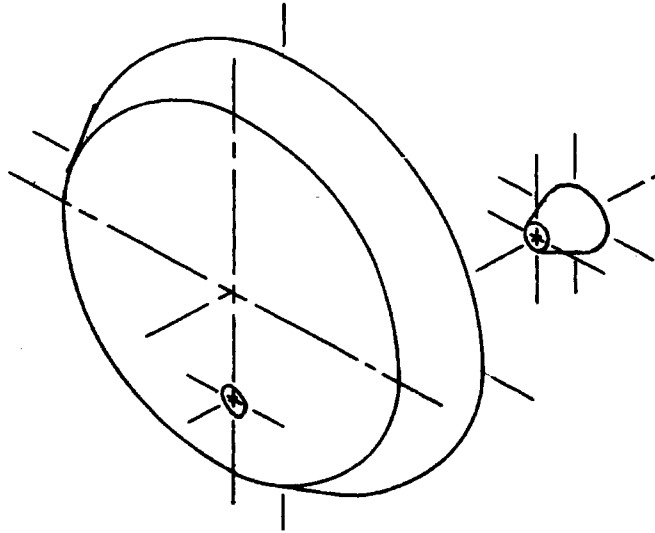
a.   Interferometer Window

b.   Schlieren Window

Figure 11.   Window Disks and Glass

also move laterally to follow the window motion.

Vertical motion of the system was provided by three hydraulic jacks. Each jack had a lifting capacity of one and one-half tons but did not support more than about 400 pounds. To keep disturbances of the optical system at a minimum while it was being moved to follow the windows, the jacks were, mounted directly above the casters. Thus the necessity for lowering the jacks before each move was eliminated. The hydraulic jacks allowed the elevation and level of the system to be accurately controlled while providing a slight shock absorber effect.

All three casters, of the swivel type, provided excellent maneuverability, but they could not be loaded directly over the axle. The moment created by this eccentric loading was counteracted by three one inch diameter guide rods which slid up and down in pipes welded to the base (Figure 12). The entire support assembly above each caster consisted of an 8 x 8 x 1/2 inch steel plate to which the hydraulic jack and guide rods were bolted and welded respectively. This assembly mated with a leg welded under the main H-beam. Each leg was a four inch length of H-beam. The guide pipes, welded inside the leg, protruded through the lower flange of the main beam. A hole was also cut in the beam to allow the head of the jack to bear on a block which was welded to the web of the H-beam. The minimum height of the base was thus sixteen and one-half inches from the floor to the top of the main H-beam.

Figure 12.   Mobile Base Leg

The configuration of the support structure was designed to match the configuration of the interferometer. The optical benches which weigh about 150 pounds each will be bolted to the base on the 1/2 x 3 x 12 inch steel pads provided. The bench arrangement (Figure 9) will distribute the total load nearly equally to the three wheel locations. Dowelled and bolted joints will maintain the proper alignment of the optical benches. The laser will rest on a raised platform to assure that its axis coincides with the interferometer's optical axis.

The schlieren system used was built by Philip Chen (1) and is fully described in his thesis. It was a twin mirror system employing two parabolic concave mirrors and three front surface plane mirrors to make up the configuration of Figure 13. All these parts were mounted on a plywood chassis, a box 8 inches in height and depth and 96 inches long. The image cut-off device, also attached to the chassis, embodied adjustments to focus the second parabolic mirror in the plane of the knife-edge and to move the knife-edge with horizontal, vertical and rotary motion. Transverse motion at any particular angular orientation was also possible.

The recording device was a Graphflex Photorecord, 35 mm camera from which the lens and shutter system had been removed. The shutter was mounted at one end of an aluminum tube in which a telescope objective lens had been fixed. This is designated as the high power telescope in Figure 13. Adapting the camera to the other end of the tube gave the camera a 31 inch effective focal length. Figure 14 is a photograph of the camera in place on
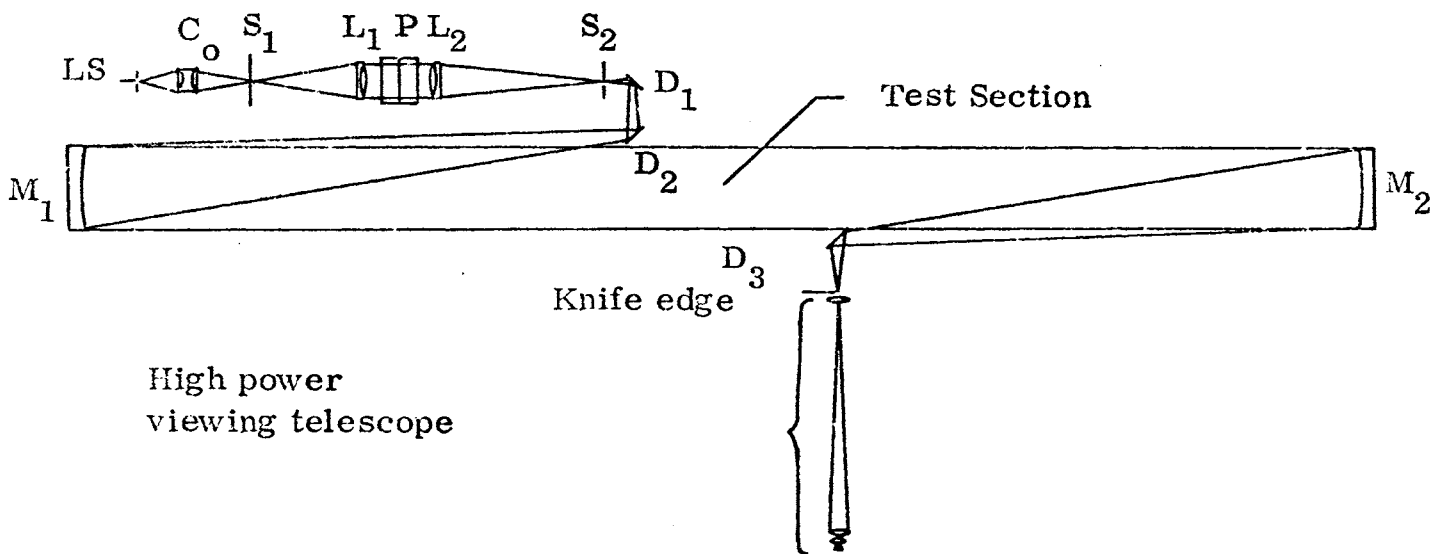
LS	Light source	P	Prism
C_o	Condenser	L_2	Telescope lens
S_1	First Slit	S_2	Second Slit
L_1	Collimator	D_1, D_2 & D_3	Diagonal Mirrors
M_1 & M_2	Parabolic Mirrors		

Figure 13.   Schematic Diagram of Twin-Mirror

Schlieren System
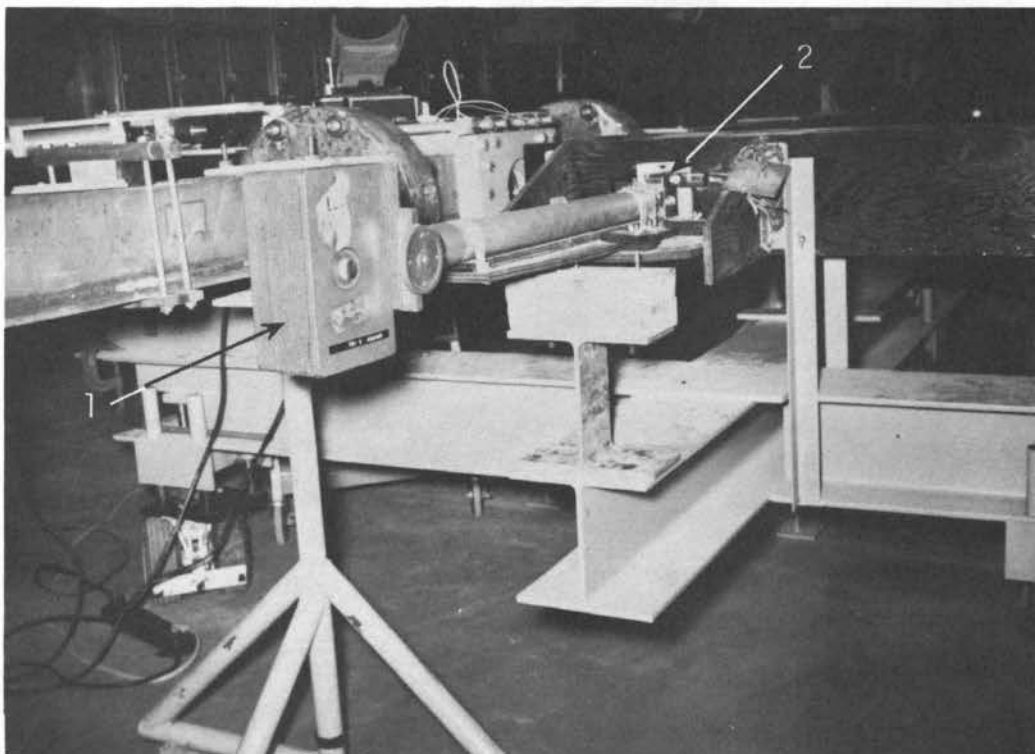
1. Camera for Schlieren System

2. Image Cut-Off Device

   Adjustments K_1, K_2 and K_3

Figure 14.   Schlieren System on Mobile Base

the telescope. The image cut-off device is also visible.

The light source used was an electronic flash lamp, Honeywell Strobonar Model 660, with a minimum light pulse duration of about 20 microseconds. It was bolted to the schlieren system chassis by the bracket directly behind the oscilloscope in the photo of Figure 10. The front face of the lamp was positioned in the same plane that the filament of a continuous light source occupied during the aligning procedure.

Triggering for the flash lamp was provided through a silicon control rectifier (G.E. C20C). The SCR gate was triggered by the external delayed trigger source from the time delay circuit built into the oscilloscope which was used for these experiments. This delay circuit was continuously calibrated for delay times from 0.1×10^{-6} seconds to 50 seconds. The light pulse from the flash lamp occurred less than one microsecond after the trigger pulse from the delayed trigger.

The schlieren system was mounted on the mobile base allowing the shock tube test section to pass through the collimated portion of the beam (Figure 10). The end of the system to which the light source was attached was set atop an H-beam section which was then clamped to the mobile base. The other end was bolted to the laser platform supports and the camera was supported by another short length of H-beam. All slits of the light source system were in a vertical position.

To permit the use of the optical systems, arrangement was made to mount glass windows in the shock tube walls. The four inch diameter windows

used with the schlieren system are shown in the photograph of Figure 15.

Drawings 1 through 5 in Appendix II are detail drawings of the parts used to

hold the schlieren windows in place. The window glass, fused silica, was

secured in the window disks (Drawing No. 2) which were in turn secured in

the mounting plates (Drawing No. 1) by the cover plates (Drawings No. 4 and 5).

The mounting plates were bolted to each other across the shock tube. Because

of the difference in optical requirements and beam size in the schlieren and

interferometer systems, provision was made in the window design for the

interchange of window disks. One set holds the schlieren windows while the

other set will hold the smaller interferometer windows. Drawing No. 6 gives

the basic dimensions of the latter. Changing from one system to the other

does not require actually handling the glass since it can remain in the window

disks.

The schlieren windows were one inch thick and accommodated a beam

diameter of about four inches. Each piece of glass fit in a tapered hole in

the steel window disks (Drawing No. 2). The schlieren window hold down ring

(Drawing No. 3) pressed the glass tightly into the hole against an 0-ring and

thus sealed the opening with the surface of the glass flush with the inner sur-

face of the window disk. Twelve, 5/16 - 24 UNF bolts held each schlieren

window in place. To assure an even clamping pressure on the glass, a

tightening torque of one hundred inch-pounds was applied to each bolt. The

schlieren window was mounted 5/16 inch off-center so that the glass could

overlap the top or bottom edge of the shock tube. Thus, optical studies
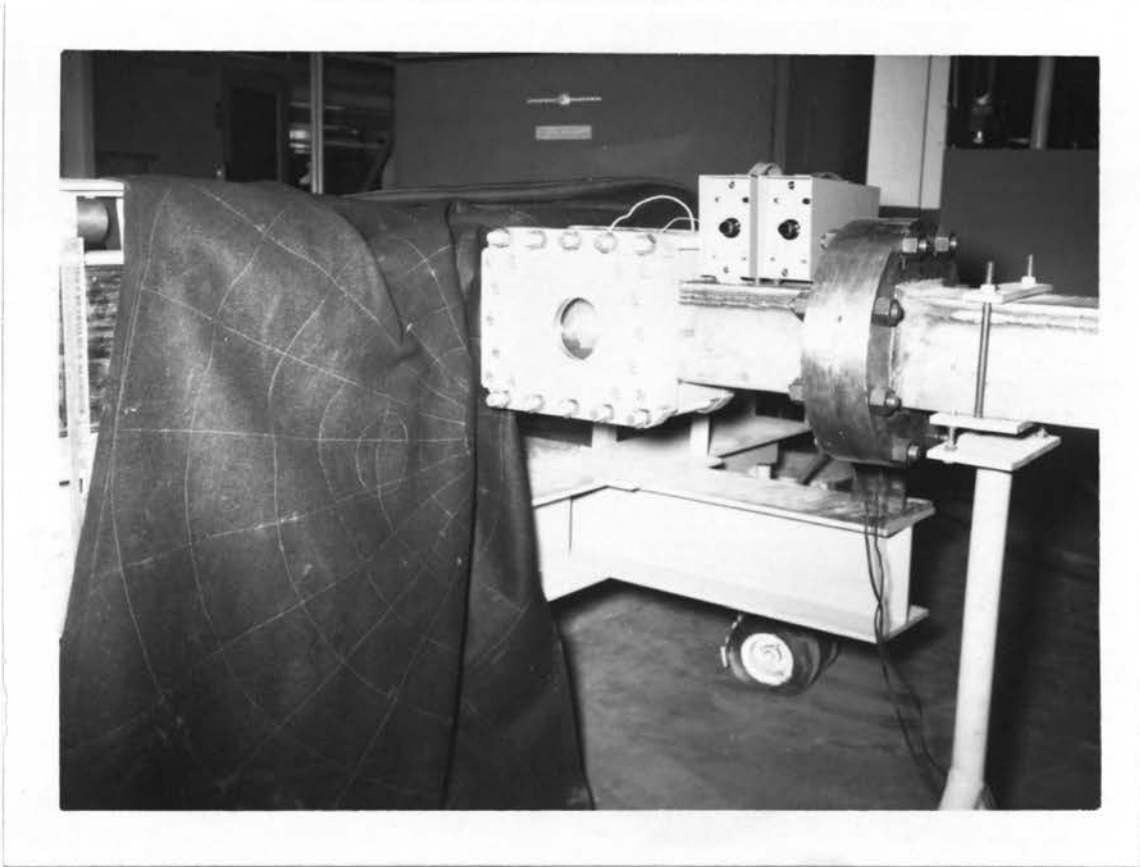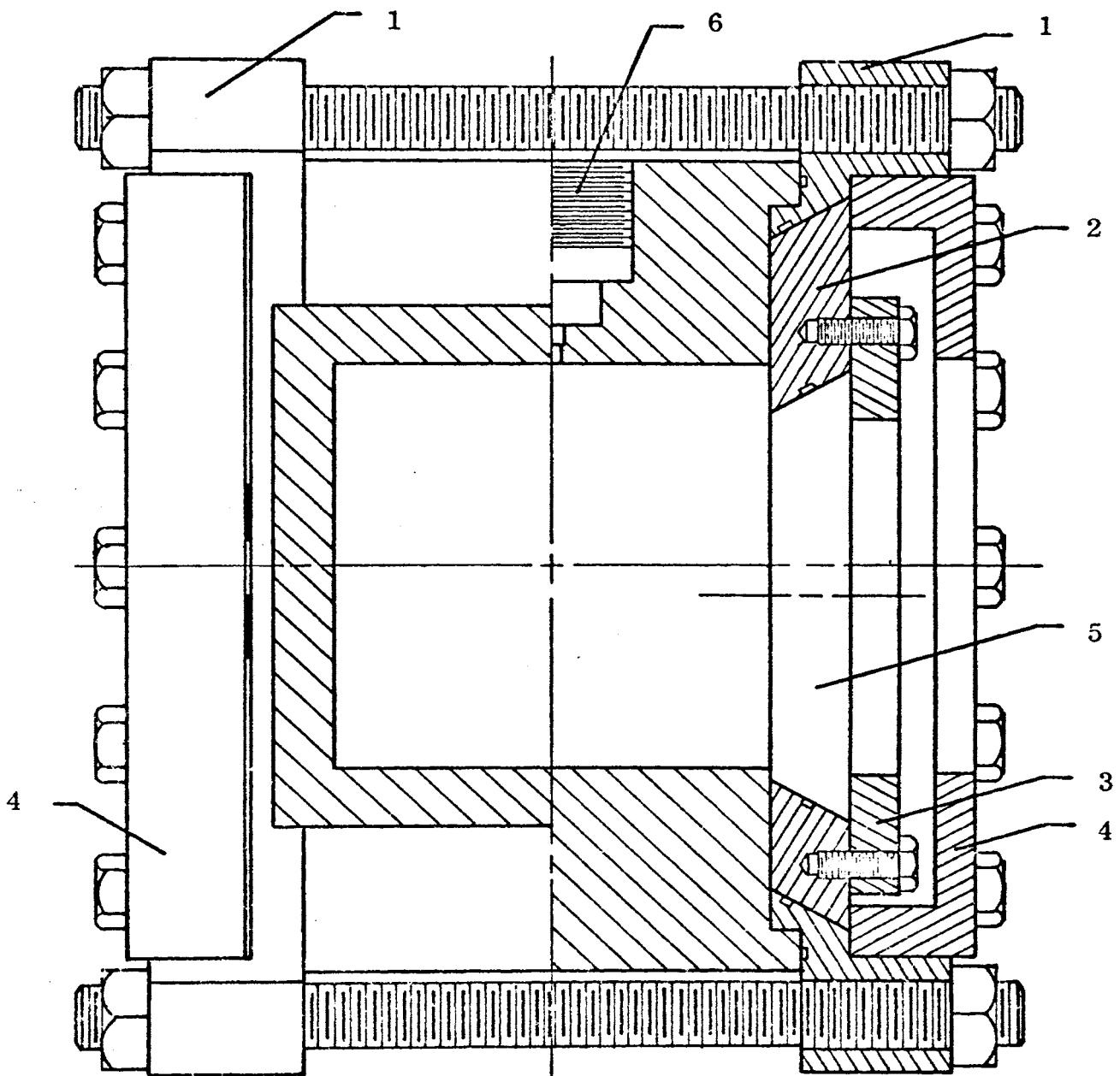
Figure 15.   Shock Tube Window Mounts

could be made at any vertical position in the shock tube. The size of the schlieren window and its hold down ring required the cover plate to be assembled in one particular orientation with respect to the window. To traverse the entire tube cross section, the cover plate would need to be rotated along with the schlieren window through a full 180 degrees.

The interferometer windows were 3/4 inch thick and the surfaces were ground flat and parallel to within 1/10 wavelength. The maximum beam diameter which could be used with these windows is about 3/8 inch. Mounting these windows off-center will allow the entire vertical cross section of the tube to be accessible to the interferometer. The window size and off-set will cause the windows to travel in an arc as the disk is rotated, rather than moving directly vertically. Index marks on the cover plates will aid in alignment of the windows during the rotation.

The mounting plates were used to provide support for the windows and cover plates. By bolting the mounting plates to each other, a firm support for the windows was provided. Having the small diameter of the tapered hole to the inside of the tube allowed the window disks to be inserted or removed without removing the mounting plates from the tube. The arrangement was good for vacuum purposes as the lower pressure inside the tube aided in sealing the opening by more secure seating of the disk. Also, no bolts or fasteners were required inside the tube. The cover plate, when bolted to the mounting plate, pressed the window disk into the tapered hole against an 0-ring and flush with the inside of the tube. An offset section view through

1. Mounting Plate   4. Cover Plate

2. Window Disk   5. Window Glass

3. Hold Down Ring   6. Transducer Adapter Hole

Figure 16.   Offset Section Through

Window Assembly

the window assembly on the shock tube is shown in Figure 16.

At the beginning of each experiment, a vacuum was drawn on the tube. The glass was then supported by its tapered hole. After the shock had passed the window, a residual positive pressure was left in the tube until vented to the atmosphere. During this time the glass was held in place by the hold down rings; the window disks were held in place by the cover plates and the mounting plates supported the entire load through the connecter bolts. Sample calculations in Appendix II show that all bolts were selected to withstand internal tube pressures over 4000 pounds per square inch. However, the schlieren window hold down ring in its present form (Drawing No. 3) should not be subjected to pressures greater than about 1300 pounds per square inch.

The large bearing surface necessary for the 0-ring seal behind the mounting plates was obtained by welding a steel block on the top and bottom of the shock tube (Figure 17). After welding, the sides of the tube were machined parallel and to a thickness of 5/16 inch. A seven and seven-eighths inch diameter hole 5/16 inch deep then just reached the inside of the tube wall and the mounting plates did not protrude into the flow path.

A photograph of the shock wave does not answer all the questions required to study thoroughly the shock wave. Velocity determination using shock wave detectors which do not obstruct the flow is necessary. In early shock tube investigations, the detectors most frequently used were thin film resistance gauges which had a very good response to temperature changes. Calorimeter or thick film heat gauges (15) were also developed to measure
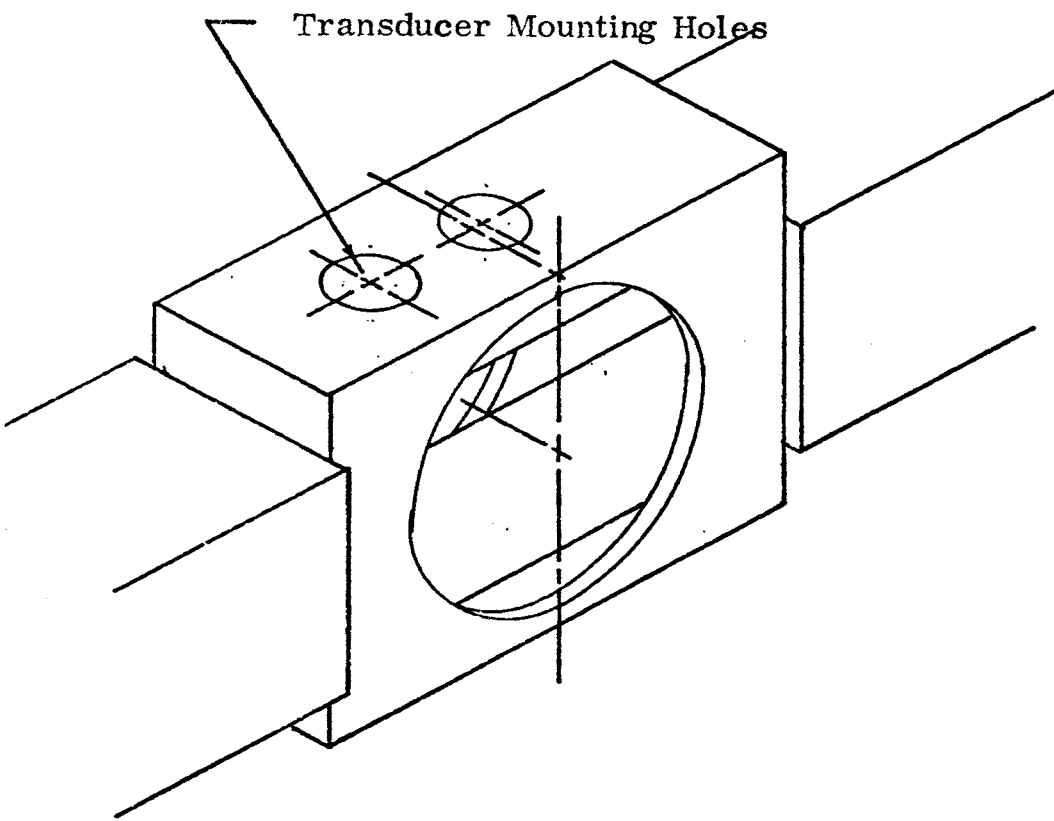
Transducer Mounting Holes

Figure 17. Shock Tube Modification

high heat transfer rates more accurately than the thin film gauges. The development of piezo-electric crystals to measure dynamic pressure changes had made the measurement of pressure in the shock tube more feasible. Crystals with output rise times of about three microseconds are much better shock detectors than mechanically activated pressure sensors. The crystals are also easier to operate and maintain than the thin film gauges.

For this facility, the decision was made to use two piezoelectric pressure transducers, Kistler Model 601A, and flush-mount them in the top of the shock tube. A velocity determination was made from the time interval between pressure transducer outputs and was the average velocity over the distance between the pressure transducer locations. Because of the attenuation of shock velocity and strength which occurs in the length of the tube, the accuracy of the velocity calculation is greatly affected by the separation of the transducers. The more closely they can be mounted to each other, the more accurate the velocity determination for that position in the tube will become.

The transducers for this facility were mounted in the shock tube by first mounting them in stainless steel adapters (Drawing No. 7, Appendix II) which were screwed into the appropriate holes in the top of the shock tube (Figure 17). One hole was located two and three-quarter inches upstream (toward the diaphragms) from the center of the mounting plates. The other hole was one-quarter inch downstream of the same centerline, making the total separation 3.000 ± .005 inches. All optical studies could thus be made between the transducer locations. The output of the first transducer

was then used to trigger the light source for the schlieren system.

J. C. Muirhead's (13) experience with pressure transducer mountings in shock tubes showed that his method of mounting the transducer on its own base, separated from the shock tube, yielded a pressure trace free from disturbances caused by shock tube vibration. The transducer was mounted in a large mass and suspended in a hole in the shock tube. This method has its advantages, but it was not practical in this facility primarily because of the location of all the optical equipment. Observation of the pressure traces, such as those shown in Figure 18, page 50, indicated that the transducers were not subjected to a significant amount of tube vibrations.

IV. EXAMPLE EXPERIMENTAL PROCEDURE

The equipment used for these experiments included the shock tube (4), schlieren system (1), the Kistler Model 601A pressure transducers with charge amplifiers, and the Tektronix Dual Beam Oscilloscope, Model 556, with polaroid camera. Helium was the driver gas for all runs in this series.

Step one in preparing for a run in the double diaphragm mode was to align the schlieren system using the procedure described in Appendix I, or to verify the alignment of the system. This time was also used as warm-up time for the electronic equipment.

Following the optical system alignment, a diaphragm was inserted between the test section and driver section and evacuation of the tube was begun.

An estimate of the shock velocity and strength was made by reference to charts on double diaphragm shock tube theory which determine the expected resultant Mach number as a function of the pressure ratios between the various sections of the tube. One such chart was available from Mr. H. S. Joyner's work (11). The necessary trace sweep rate for the oscilloscope and required amplifier gains were determined. The estimate of shock velocity also provided a basis on which to calculate the approximate delay time necessary for the light trigger.

After a sufficient warm-up period, the charge amplifiers were checked for zero and drift and the controls of the oscilloscope were set to the desired positions. For recording the pressure traces, both beams of the scope made a single sweep at a rate set by the common time base. The output from the

first pressure transducer triggered the sweep of both beams simultaneously. A data sheet (Table I) on oscilloscope settings, charge amplifier settings and diaphragm dimensions was completed for all tests.

With all controls set as desired, the sweep triggering level was adjusted to eliminate accidental triggering by a switch which could be used to initiate diaphragm rupture. The switch activated a solenoid to release a spring loaded plunger which would strike the diaphragm initiating the rupture. The triggering level having been set, the plunger was cocked and the switch unplugged. The second diaphragm was then positioned without danger of accidental plunger release.

With these final settings made, the oscilloscope and light operation were checked by triggering the single sweep with the calibrated output from the oscilloscope.

After this check, the oscilloscope grid was photographed and the grid illumination was turned off. The test section pressure was recorded and the valve to the vacuum pump was closed to protect the vacuum gauge. The oscilloscope sweep was armed and the camera shutters were opened for a time exposure as pressure was increased in the driver section. This procedure assured recording of data regardless of whether the diaphragm was ruptured at a predetermined pressure or ruptured under pressure before the desired value was reached.

Immediately after the rupture of the diaphragm the camera shutters were closed and the residual pressure in the tube was read and recorded.

TABLE I

EXAMPLE TEST DATA

Pressures:

Test Section	1/4 in Hg.
Primary Driver	335 psig
Secondary Driver	29 in. Hg
Resultant	43-1/2 psig

Diaphragms:	Total Thickness (in.)	Scribe Depth (in.)	Resultant (in.)
Primary	.085	.020	.065
Secondary	-.085	.050	.035

Oscilloscope Setting:

Beam	A	B
Intensity	6-1/2	6-1/2
Display	Left Plug In	Right Plug In
	B	B
Display Magnitude	x1	x1
Mode	Single Sweep	Single Sweep
Trigger	Left	Left
Source	Internal Plug In	Internal Plug In
Coupling	AC	AC
Slope	+	+
Time/cm	$10\ \mu$ sec/cm	$10\ \mu$ sec/cm
Pre amp	0.1 volts/cm	0.1 volts/cm
Charge Amplifier	10 mV/pCb	10 mV/pCb

Photographs:

Oscilloscope: Polaroid Type 47 ASA 3000

	Scale Illumination	f Stop	Shutter Speed
Scale	7	5.6	1/5 sec
Signal	0	5.6	Time

Schlieren: Kodak Tri X Pan ASA 400

Shutter Speed – Time

Flash Duration – $20\ \mu$ sec

The pressure was then released slowly and the diaphragms were removed.

Pressure and velocity calculations were made from the polaroid picture of the pressure traces.

RESULTS OF EXAMPLE

The photograph of Figure 18 is a typical pressure transducer output trace displayed by the oscilloscope and was photographed during the run for which the data of Table 1 was recorded. The upper trace was the output of the first transducer which was positioned upstream from the windows. The lower trace was the output of the second transducer positioned directly over the window. The velocity was determined by measuring the horizontal distance from point 1 to point 2 on the photograph and multiplying by the sweep rate to determine the elapsed time. Point 2 is a point on the initial pressure output of the second transducer which corresponded in voltage level to the voltage level required for the first pulse to trigger the trace sweeps.

The elapsed time over the distance of three inches for this run was

$$4.25 \text{ cm} \times 10 \mu\text{sec/cm} = 42.5 \mu\text{sec}.$$

The velocity was then

$$\frac{3 \text{ in.}}{12 \text{ in/ft} \times 42.5 \times 10^{-6} \text{ sec.}} = 5890 \text{ ft. per sec.}$$

Sonic velocity, c, in the tube with air temperature of $80^{\circ}F$ was calculated by the formula

$$c = \sqrt{\gamma g_c R_g T}$$

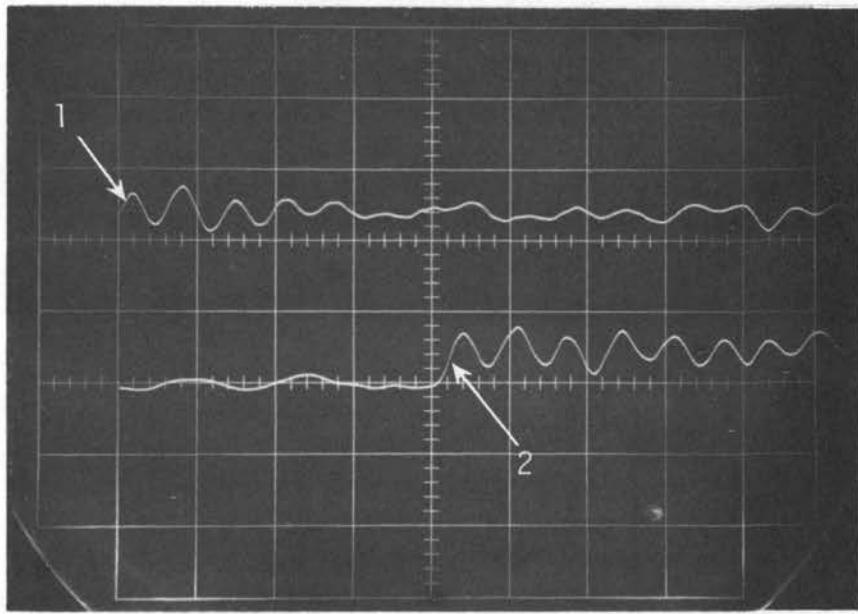where γ is the ratio of specific heats, R_g is the specific gas constant for

Figure 18.   Pressure Transducer Trace

air, 53.3 (ft-lb$_f$)/(lb$_m$-^{o}R), g$_c$ is the gravitational constant, 32.2 (lb$_m$-ft)/ (lb$_f$-sec^2); and T is the temperature in degrees Rankine. Thus,

$$c = \sqrt{1.4 \ (32.2) \ (53.3) \ (540)} = 1138 \text{ ft/sec}$$

The Mach number, shock velocity divided by sonic velocity, was

$$M_A = \frac{5890 \text{ ft/sec}}{1138 \text{ ft/sec}} = 5.17$$

Static pressure measurement from the pressure traces was rather inaccurate because both transducers apparently vibrated at their natural frequency following excitation by the step input of the pressure pulse. The lower trace appeared as an undamped sine wave oscillating at 150 kilocycles per second while the upper trace displayed "beats" or alternating periods of resonant and attenuated vibration. This oscillatory response is a typical reaction of any undamped or lightly damped system to a step input. The output charge oscillates about the value of the pressure induced charge level.

The pressure calculation was made by finding an average voltage level of the first few oscillations of the two traces. The scale factor or vertical amplifier gain in the oscilloscope for this run was 0.1 volts per centimeter and the average output was determined to be 0.04 volts. This reading divided by the charge amplifier gain, 10 millivolts per picocoulomb, determined the charge output of the transducers at

$$\frac{40 \text{ mv}}{10 \text{ mv/pCb}} = 4 \text{ picocoulombs}$$

Dividing the charge by the calibration sensitivity of the transducer, 1.12 pCb/psi determined the magnitude of the static pressure change

$$\frac{4 \ pCb}{1.12 \ pCb/psi} = 3.67 \ psi$$

Using the actual initial tube pressure as the zero transducer pressure reading, the static pressure ratio across the shock wave was

$$\frac{p_y}{p_x} = \frac{3.792 \ psia}{0.122 \ psia} = 31.09$$

The theoretical value of the static pressure ratio across a shock wave is most easily calculated in a reference frame which is traveling with the shock wave. This essentially makes the shock wave stationary and lets the gas flow through the discontinuity. Because the gas into which the shock wave is actually moving is at rest with respect to the tube, the gas velocity with respect to the shock wave is equal to the actual shock velocity as measured in the tube. Thus, in the reference frame attached to the shock, the velocity of the gas (subscript x) approaching the shock wave is M_x and in the test is

$$M_x = 5.17.$$

In this frame of reference, the Mach number of the gas moving away from the shock wave (subscript y) will be subsonic because of the strong normal shock and may be calculated by the equation

$$M_y^2 = \frac{M_x + 2/(\gamma - 1)}{2\gamma/(\gamma - 1) \ M_x^2 - 1}$$

where again γ is the ratio of specific heats.

$$M_y^2 = \frac{(5.17)^2 + 2/0.4}{(2.8/0.4) \ (5.17)^2 - 1} = 0.1708$$

This value of M_y^2 can be substituted directly into the equation

$$\frac{p_y}{p_x} = \frac{1 + \gamma M_x^2}{1 + \gamma M_y^2}$$

to calculate the static pressure ratio across the shock wave. The calculated ratio is then,

$$\frac{p_y}{p_x} = \frac{1 + 1.4(5.17)^2}{1 + 1.4(.1708)^2} = 31.82$$

The experimental value is very close to the theoretical value considering the technique required to read the vacuum gauge and the oscilloscope traces. The equations used for the theoretical calculations were taken from Chapter 5 of A. H. Shapiro's Book (18).

V. GENERAL RESULTS

The mobile base was subject to reaction to some low frequency vibrations, but no apparent effects were transmitted to the schlieren system. Since the two ends of the schlieren system were not rigidly attached to each other through their own chassis, one end could be moved relative to the other. The alignment was not permanently affected by any applied force on the mobile base. The mobile base thus displayed its capability to isolate the system from high frequency vibration and to provide the required rigidity and mobility.

Window performance was excellent. The seal performance was demonstrated by the very low pressures reached with the vacuum pump on the tube. Once the valve to the vacuum pump was closed, the tube pressure increased at a rate less than two inches of mercury per hour; a quite acceptable leak rate for this series of tests.

No static test was performed on the windows to determine maximum safe working conditions and at no time during this series of tests was the test section subjected to a static pressure of more than 70 pounds per square inch. Higher pressures will occur as higher Mach numbers are obtained, however, the use of combustion techniques should still limit the internal tube pressure to the design pressure of 1000 psi. At this pressure, all parts of the window mounts with the exception of the schlieren window hold down ring have a design factor of safety of from four to about six. The schlieren window hold down ring was limited to 1345 psi static tube pressure as shown by the calculations in Appendix II.

The mounting plates were subjected to some bending when the connector bolts were tightened. Since this could have resulted in a poor seal, the cover plates were tightened into position before final tightening of the connector bolts. The inner surface of the cover plate did not fit exactly flat against the mounting plate because a shim was used on the outer edge of the window disks to increase their thickness and improve clamping pressure on the disk. This allowed shims to be placed between the cover and mounting plates on both sides of the bolts which were at the level of the tube centerline (Figure 16). Securely tightening the cover plate bolts therefore acted to bend the mounting plate in the opposite direction from the connector bolts. The net effect was to hold the mounting plates straight and relieve stresses due to bending in the thinnest portion of the mounting plates. The shock tube test section was also greatly stiffened by the addition of the window assemblies.

Pressure transducer output could be adequately interpreted by averaging the voltage output of the traces. However, the oscillatory nature of the traces was undesirable. Various settings of amplifier gains and different shock velocities failed to have any effect on the nature of the two traces. Setting the gains too high resulted in pressure traces which could not be used for pressure calculations because the traces were not bright enough at the very fast sweep rates to expose properly the recording film. Approximate velocity measurements, within 5 to 10 percent error, could be obtained because film exposure was sufficient on the second trace up to the point of trace deflection caused by the pressure pulse.

The photograph of Figure 19 is a steady state schlieren picture of a heated soldering iron. The soldering iron tip extends from the right side of the photograph towards the upper left hand corner and in this print is about one and one-half times its actual size. On the right side of the picture is shown a wire which was hanging across the center of the shock tube windows as a reference marker. Thus the position of the soldering iron is indicated for this photograph as being nearly in the center of the schlieren window. The tip was actually held outside the windows with the tip pointing generally in the direction of the driver sections of the tube. Illumination for the photograph was provided by a single flash from the flash lamp with light duration of approximately 20 microseconds.

The useful size of the schlieren field was severely limited by shadows of two diagonal mirrors, thus reducing the margin for error in setting the delay time multiplier for the flash lamp delay trigger. In order to get a picture of the shock wave, the velocity had to be predicted quite closely because the free field under these conditions was limited to about 2 inches along the tube length instead of the 3 to 4 inches desired. No schlieren picture of the shock wave was obtained during this series of runs due first to inaccuracy of timing and then to failure of the triggering switch for the light source.

Figure 20 is a photograph of some of the diaphragms used during this series of tests. All diaphragms were cut from aluminum sheets 0.085 inches thick. The material was quite ductile and no breakage occurred in the shock tube. Figure 21 is the bursting pressure data obtained from the tests conducted. All scribing was done with a milling machine and the best results

Figure 19.   Steady State Schlieren Picture
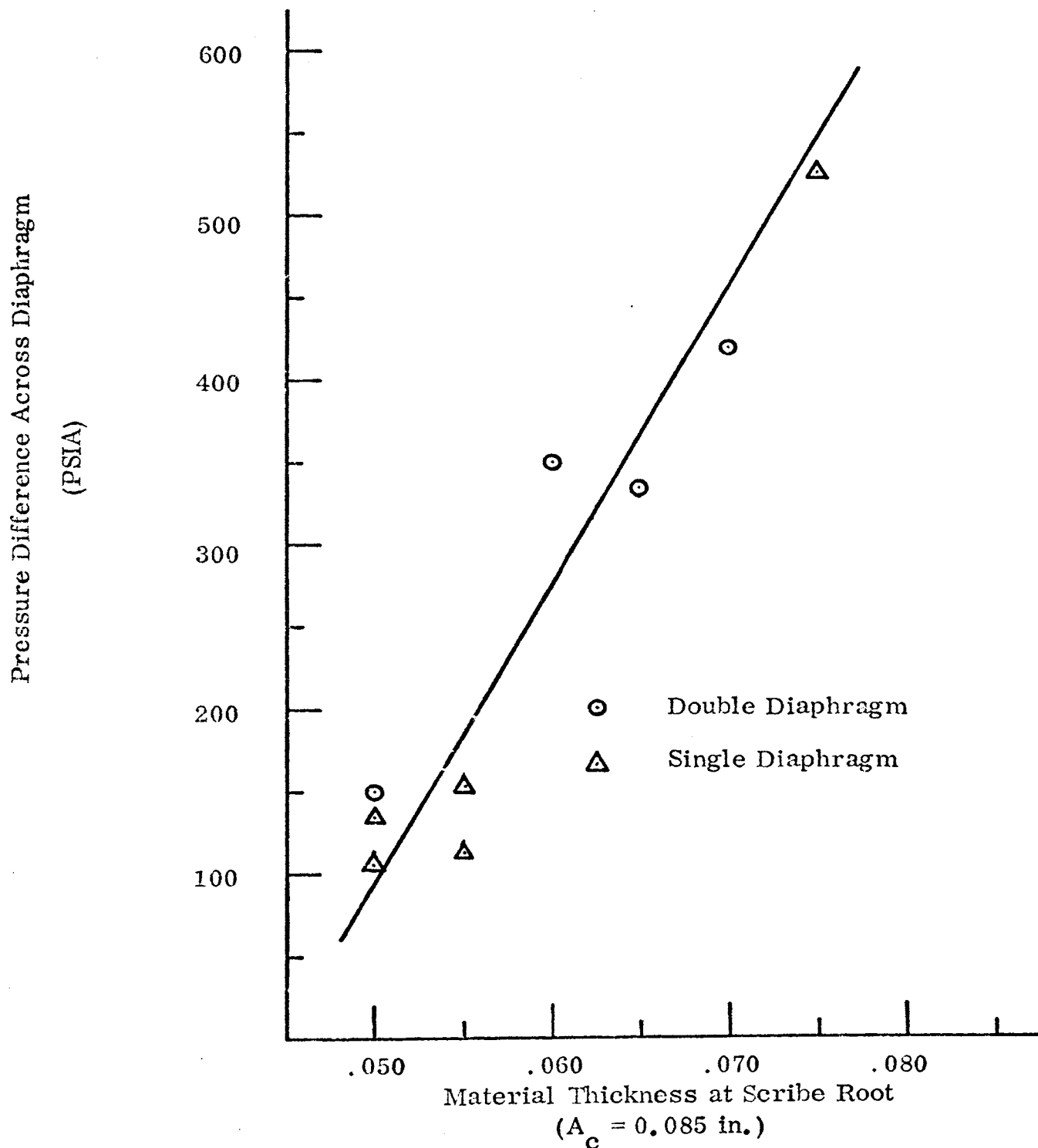of Heated Soldering Iron

Figure 20. Ruptured Diaphragm

Figure 21. Diaphragm Bursting Pressure Data Versus

Material Thickness at Scribe Root

were obtained from diaphragms scribed by an end mill with the milling head at 45° to the plane of the working table. All scribe marks were made at 45° to the rollmarks on the material. Difficulty was encountered with some diaphragms which were not absolutely flat before scribing because the scribe depth varied and the petalling effect was not uniform or predictable. The line drawn on the graph of Figure 21 is a random line to indicate the general trend in the data.

During this series of tests the facility was operated in both single and double diaphragm modes. Mach numbers which were recorded during the series varied from about 4 to 5.25 and were in general agreement with theory when the area changes of the tube were taken into account along with the pressure ratios. Evidence from these tests indicated that producing a shock wave of low velocity was more difficult than expected. Single diaphragm operation and only partial evacuation of the tube might be used to obtain the low Mach numbers.

VI. CONCLUSIONS AND RECOMMENDATIONS

The mobile base and windows which were designed and built by the author performed their intended functions very well. To make the windows safer, however, the schlieren window hold down ring should be rebuilt to about twice the present thickness. The result would be to raise its factor of safety by nearly four hundred percent.

The transducers and amplifiers worked properly, but the absolute pressures measured were very low compared to the 0 to 5000 psi range of the transducers. Possible use of crystals with a lower pressure range ought to be investigated. This type of change, or some external circuitry to add electrical damping to the signal might improve the readability of the pressure traces. The accuracy of the velocity determination is very dependent on the accuracy of the physical measurement of the distance from point to point on a photograph. The use of a digital interval counter with minimum divisions of 0.1×10^{-6} seconds would improve the accuracy by providing a direct reading of the interval that must be measured in the photograph.

Improvements to the schlieren system should be a light source with light pulse duration of about 1 to 5 microseconds. A purchased or developed source of this duration would extend the useful range of the schlieren system into the higher Mach numbers. A reliable switch for the light trigger must also be used. Efficient use of any light source is necessary for good photographic results. For a given light source, one particular color of the spectrum may be brighter than the other colors. Experimentation with the focusing of the schlieren system

should determine the procedure necessary to allow any color of the spectrum to be used as the green light was in these experiments.

The diaphragm material was very good. One recommendation in its use would be to develop a system or method to insure uniform scribe depth on each diaphragm. With more uniformity of the scribe depths, the bursting pressures should become more predictable and reproducible.

Because no results are immediately available from the 35 mm camera now used with the schlieren system, any errors in alignment could go undetected during a series of tests. The addition of an adapter to mount a polaroid camera in place of the 35 mm camera on the schlieren system would shorten the time necessary to evaluate a test's results. If adjustments were necessary, they could be made after each test.

VII. BIBLIOGRAPHY

1. Chen, P.L., Temperature Distribution in Thermal Boundary Layers (in Free Convection) Using a Modified Schlieren Method, Thesis, University of Missouri at Rolla, (1965).

2. Chesterman, W.D., The Photographic Study of Rapid Events, Oxford of the Clarendon Press, (1951).

3. Cole, J.K.,"Spark Gap Development", Reprint by Sandia Corp., No. SC-R-64-119, (1964).

4. Crede, W.A., The Design and Construction of a Shock Tube Facility, Thesis, University of Missouri at Rolla, (1965).

5. Den Hartog, J.P., Advanced Strength of Materials, McGraw Hill Book Co,, Inc., 100 (1952).

6. Frungel, F., High Frequency Flash Lamp, Proceedings of the Third International Congress on High Speed Photography, Academic Press Inc., New York,57 (1956).

7. Hills, H.F., Layout and Details of the Multiple Spark Range at Cambridge, Proceedings of the Third International Congress on High Speed Photography, Academic Press Inc., New York, 279 (1956).

8. Hyzer, W.G., Engineering and Scientific High Speed Photography, The Macmillan Co., New York, (1957).

9. Jenkins, F.A., and White, H.E., Fundamentals of Optics, McGraw-Hill Book Co., Inc., New York, (1957).

10. Jones, G.A., High-Speed Photography, John Wiley and Sons Inc., New York, (1952).

11. Joyner, H.S., Iionization of Air Produced by Strong Shocks, Thesis (in preparation), University of Missouri at Rolla, (1968).

12. Looms, J.S.T., and Smith, R.J., Short Duration Spark Light Source for Photography of High-Speed Airflow, Proceedings of the Third International Congress on High Speed Photography, Academic Press Inc., New York, 62 (1956).

13. Muirhead, J.C.,"Mounting Pressure Transducers in Shock Tubes", J. Sci. Instr., 39, 447 (1962).

14. Parks. E.K., and Petersen, R.E.,"A Versatile Shock Tube Facility", EES Report No. 3, The University of Arizona, Tuscon, (1963).

15. Rose, P.H., "Development of the Calorimeter Heat Transfer Gauge For Use in Shock Tubes", Avco Research Laboratory, Report 17, (1958).

16. Schardin, H., High-Frequency Cinematography in the Shock Tube, Proceedings of the Third International Congress on High Speed Photography, Academic Press Inc., New York, 365 (1956).

17. Schardin, H., Ergebnisse der Exacten Naturwissenschaften, 1941, 20.

18. Shapiro, A.H., Dynamics and Thermodynamics of Compressible Fluid Flow, Ronald Press, New York, 59 (1953).

19. Shigley, J.E., Mechanical Engineering Design, McGraw-Hill Book Co., Inc., 234 (1963).

20. Temple, E.B., "Quantitative Measurement of Gas Densities By Means of Light Interference in a Schlieren System", Journal of the Optical Society of America, 47, No. 1, 91 (1956).

21. Theophanus, G.A., "Spark Light Source For Schlieren Photography", R. Sci. Instr., 36, 550 (1965).

22. Tolansky, S., An Introduction to Interferometry, Longmans, Green and Co., London, England, (1955).

APPENDIX I

PROCEDURES FOR USING THE TWIN-MIRROR SCHLIEREN SYSTEM (1)

1)   Light Source System (Refer to Figure 13)

First, adjust the position of the condenser along its optical axis to form a sharp image of the light bulb filament at the plane of the first narrow slit (S_1) and then adjust the position of the image of the filament to the center of the slit by turning the three screws at the bulb socket base. The distance between the first slit and the collimator is fixed at 178 mm, exactly one focal length of the collimator. Remove the prism and turn the system to place every optical part on one common optical axis. This position can be easily seen if the image of the first slit falls on the second slit (S_2) which was centered previously. The next step is to adjust the focus of the telescope objective lens (L_2) to form a clear image of the first slit on the plane of the second slit (S_2). Move the movable arm of the light source system to about 30 degrees and insert the prism into the system. Then adjust the movable arm to make the spectrum fall on the second slit (S_2). The prism should be placed symmetrically to both incidental light and refracted light.

2)   Diagonal Mirror D_1 and D_2

Put the complete light source system in place and adjust the distance from the second slit (S_2) to the first concave mirror (M_1) to exactly one focal length (45 inches). Apply the light source, and place a piece of white cardboard, about 7 by 7 inches square with a 4 inch diameter circle centered on it, in front of the first mirror (M_1). This shows if the light from the second slit

(S_2) impinges on the first concave mirror (M_1); if not, adjust the diagonal mirrors (D_1 and D_2) to make the light spot coincide with the 4 inch circle with approximately a one-half inch margin.

3)   First Concave Mirror M_1

The adjustment of the first concave mirror can be achieved by placing the same white cardboard in front of the second concave mirror (M_2) to see if the 4 inch light beam from the first concave mirror (M_1) exactly coincides with M_2; if not, adjustment of the first concave mirror is achieved by turning the three adjusting screws at the end of the box.

4)   Second Concave Mirror M_2

Insert a small piece of white cardboard between M_2 and the third diagonal mirror (D_3) to see if the reflected light from the mirror M_2 impinges at the center of the third diagonal mirror. Adjust the mirror by the three screws at the end of the box.

5)   Focusing the Second Concave Mirror (M_2) (Refer to Figures 13 and 14)

Place a small ground glass at the plane of the knife-edge and move the third diagonal mirror by turning the focusing knob K_1 to make a sharp image of the light source slit on the ground glass. The sharpness of the image can be examined by a magnifying glass. If the image is not at the center of the knife-edge, horizontal and vertical adjustment is possible by turning the knobs K_2 and K_3.

6)   Checking the Parallelism of the Knife-Edge and Image

Put the high power viewing telescope in place with a 45° viewing magnifier in place. If the knife-edge is not parallel to the light source image, turn the knife-edge.

7)   Camera Film Plane

With the camera adapter in place on the end of the high power telescope, place the ground glass in the film plane of the camera. If the entire field is not visible on the glass, adjust the position of the tube until the desired image is observed on the glass.

8)   Positioning the Flash Lamp

Measure the distance from some fixed point on the light source system to the plane of the light bulb filament used in aligning the entire system. Secure the flash lamp to its bracket so the front face of the lamp lies in the same plane that the bulb filament occupied. Observe the flash at the film plane to verify proper positioning.

APPENDIX II

WINDOW DESIGN SAMPLE CALCULATIONS

Calculations were made to assure that adequate load carrying capability was available in the bolts used to assemble the window mounts. The design pressure of the shock tube is 1000 psi, but with possible future reinforcement, the design pressure could be increased. On the basis of this possibility and the consideration of space limitations, all bolt sets were designed to have load capabilities in excess of that necessary for 4000 psi static tube pressure. Failure of the bolts is assumed to occur at the proof load or yield strength. No bolt preloading was calculated because all parts were to be sealed with 0-rings.

The connector bolts used to hold the mounting plates on the shock tube were the most critical for load carried and space required.

The first estimate of load requirements was made by using the approximate area removed from the shock tube wall and multiplying by a design pressure of 5000 psi

$$5000 \text{ psi} \times 41.55 \text{ sq. in.} = 208,000 \text{ lbs.}$$

The total force on the connector bolts was twice this figure because the bolts supported plates on both sides of the tube

$$F = 2 \times 208,000 \text{ lbs.} = 416,000 \text{ lbs.}$$

All bolts were spaced at a minimum of three and one-half bolt diameters to allow an open end wrench to be used. Knowing the length of a bolt line or bolt circle circumference, the maximum bolt diameter was calculated by

$$D_{max} = \frac{LBL}{(NB - 1) \, 3.5} \tag{II-1}$$

where LBL is the length of bolt line and NB is the number of bolts to be used on that line.

As a first trial for bolts to carry this load, select grade 5 SAE bolt material and eight bolts, four per side. With the outer of the four bolts spaced at 8.875 inches the maximum bolt diameter was by (II-1)

$$D_{max} = \frac{8.875 \text{ in.}}{(4-1)3.5} = .845 \text{ in.}$$

The load carried per bolt was

$$\frac{416,000 \text{ lbs.}}{8 \text{ bolts}} = 52,000 \text{ lbs./bolt}$$

Selecting, 0.750 - 16 UNF threads with tensile area, A_t, equal to 0.373 square inches the bolt stress, σ_b, was

$$\sigma_b = \frac{52,000 \text{ lbs.}}{0.373 \text{ sq. in.}} = 139,4000 \text{ psi}$$

This stress was much higher than the 85,000 psi proof load specified as grade 5 standard and also was greater than the ultimate strength of 120,000 psi. Therefore, eight grade 5 bolts would have been unsatisfactory for this use.

Spacing five bolts on each side over a 10.5 inch length yielded a maximum bolt diameter, by (II-1) of

$$D_{max} = \frac{10.5 \text{ in.}}{(5-1)3.5} = 0.75 \text{ in.}$$

The load per bolt then was

$$\frac{416,000 \text{ lbs.}}{10 \text{ bolts}} = 41,600 \text{ lbs./bolt}$$

Selecting grade 8 SAE material with bolt size of 0.75 - 16 UNF and $A_t =$

0.373 sq. in., the bolt stress was

$$\sigma_b = \frac{41,600 \text{ lbs.}}{.373 \text{ sq. in.}} = 112,800 \text{ psi.}$$

Since the 120,000 psi proof load for grade 8 material was greater than the bolt

stress, this bolt set was used.

When the tube contains a positive pressure, the total area subjected to

the positive pressure was the entire area within the 0-ring seal. The result

of applying pressure to this larger area with the set of bolts previously decided

upon was that the maximum safe tube pressure was decreased. The area inside

the 0-ring was

$$\frac{\pi(8.25 \text{ in.})^2}{4} = 53.33 \text{ sq. in.}$$

Using the previous bolt specifications and not adding any safety margin,

the maximum force in each bolt was:

120,000 psi x 0.373 sq. in./bolt = 45,260 lbs./bolt

Total force on the bolt set thus could not exceed

45,260 lbs./bolt x 10 bolts = 452,600 lbs.

and the maximum tube static pressure was:

$$\frac{452,600 \text{ lbs.}}{53.33 \text{ sq. in./plate} \times 2 \text{ plates}} = 4250 \text{ psi}$$

The <u>cover plate bolts</u> were designed to carry a maximum force of

$$F = \frac{\pi(7.4 \text{ in.})^2}{4}(5000 \text{ psi}) = 215,000 \text{ lbs.}$$

where 7.4 inches were the minimum diameter of the window disk. The total

tensile area of grade 8 bolt material necessary to provide a 1.2 factor of

safety was

$$A_t = 215,000 / (120,000/1.2) = 2.15 \text{ sq. in.}$$

Assuming that 14 bolts were required, the tensile area per bolt was

$$A_t = \frac{2.15 \text{ sq. in.}}{14 \text{ bolts}} = 0.1538 \text{ sq. in./bolt}$$

Bolt specification of 1/2 - 20 UNF having tensile area A_t equal to

0.1599 sq. in. met the tensile area requirements.

Because of space limitations the bolts were placed as shown on drawing

No. 4. Ninety degrees of a ten inch diameter bolt circle were used on each

side of the window opening. Spacing five bolts in these ninety degrees limited

the maximum bolt diameter to

$$\text{LBL} = \frac{90^\circ}{360^\circ} \text{x } \pi \text{ x} 10.0 = 2.5\pi \text{ in.}$$

$$D_{max} = \frac{\pi 2.5 \text{ in.}}{(5-1)3.5} = 0.56 \text{ in.}$$

which was greater than the 0.50 diameter bolts chosen. Therefore, the 14

grade 3 SAE bolts, 1/2 - 20 UNF, were used for the cover plates.

The size of the schlieren window hold down ring and the bolt set used

with the ring were closely related to obtain the smallest outside ring diameter

possible. Total force on the bolt set was

$$F = \frac{\pi (4 \text{ in.})^2}{4} (5000 \text{ psi}) = 62,8000 \text{ lbs.}$$

where 4 inches was the minimum diameter of the schlieren window glass. The

total tensile area, A_t, required to provide a factor of safety of 1.3 with grade

3 SAE bolts was

$$62,8000 \text{ lbs.}/(120,000/1.3)\text{psi} = .6804 \text{ sq. in.}$$

Assuming that 12 bolts were to be used, the tensile area per bolt was

$$\frac{.6804 \text{ sq. in.}}{12 \text{ bolts}} = .0567 \text{ sq. in./bolt}$$

The tensile area requirement was most closely matched by 5/16 - 24 UNF

bolts with tensile area A_t equal to 0.058 sq. in.

The radius to the outer edge of the hold down ring was set equal to the

maximum radius of the glass plus twice the bolt diameter (Figure II-a). Posi-

tioning the bolt circle at one bolt diameter from the outer edge allowed sufficient

bolt contact area with the ring and provided clearance between the glass and the

bolts of one half bolt diameter, (z/4).

Max. radius of glass window

Hold Down Ring

Window Disk

Window Glass
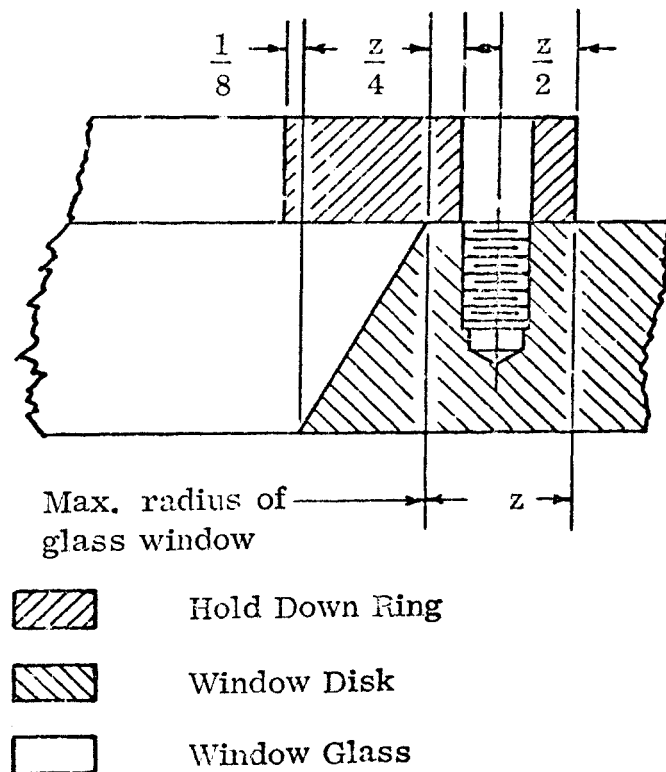
Figure II-a.   Schlieren Window Hold Down
Ring Size Determination

Inside diameter of the ring was made 1/8 inch smaller than the minimum diameter of the window design.

With the diameter of the bolt circle thus established, the maximum bolt diameter was

$$D_{max} = \frac{\pi(6.4 \text{ in.})^2}{(12-1)3.5} = 0.48 \text{ in.}$$

which was greater than the 5/16 in. diameter already chosen.

To check the load carrying capabilities of the hold down ring, (Drawing No. 3) the ring was assumed to be simply supported at the bolt circle diameter and loaded uniformly over the annular area. The maximum stress in the ring was calculated from the equation taken from page 130 of reference (5)

$$S_{max} = \lambda_i \frac{p_o R^2}{t^2}$$

where p_o is the unit load applied, R is the outer radius, and t is the thickness of the plate. The factor, λ_i, is dependent on the ratio of outer to inner radius, R/r, and is available from a chart on page 131 of reference (5).

For the conditions given

$$R/r = \frac{2.875 \text{ in.}}{1.937 \text{ in.}} = 1.483$$

and
$$\lambda_i = 0.976$$

Assuming that failure occurs at the yield point and that 50,000 psi yield point cold rolled steel was used, the maximum stress allowable with a factor of safety of 1.3 was

$$S_{max} = \frac{50,000 \text{ psi}}{1.3} = 38,450 \text{ psi}$$

The unit loading on the plate was then

$$p_o = \frac{38{,}450 \text{ psi } (.5 \text{ in.})^2}{(.976) (2.875 \text{ in.})^2} = 1192 \text{ psi}$$

This loading was assumed distributed over an area of

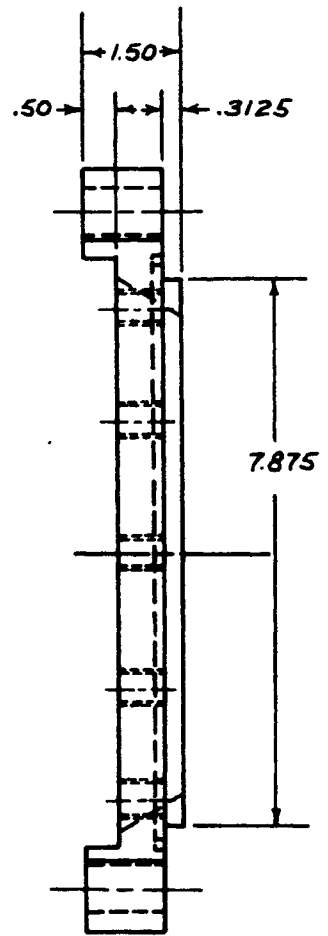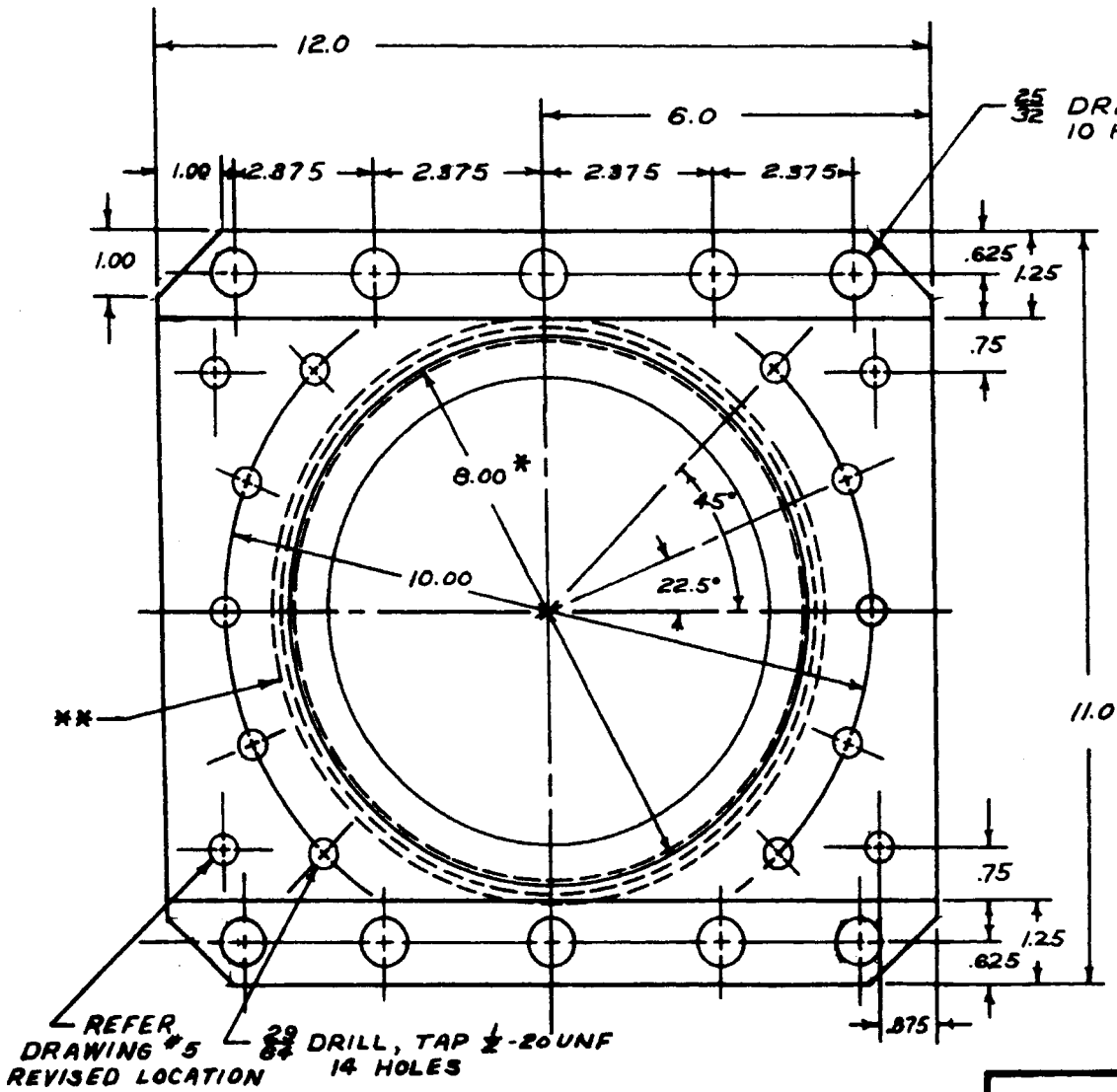$$A_L = \frac{\pi (d_o^2 - d_i^2)}{4} = 14.2 \text{ sq. in.}$$

The total force which the plate could carry was thus

1192 psi x 14.2 sq. in = 16,900 lbs.

This total force distributed over the inside surface of the glass window (d = 4 in.) represented a static tube pressure of:

$$16{,}900 \text{ lbs. x } \frac{4}{\pi (4 \text{ in.})^2} = 1345 \text{ psi}$$

Therefore, any increase in the pressure rating of the shock tube test section would require reinforcement or rebuilding of the hold down ring to maintain a reasonable factor of safety.

12.0

6.0

25/32 DRILL
10 HOLES

1.00   2.875   2.875   2.375   2.375

1.00

.625
1.25

.75

8.00 *

45°

10.00

22.5°

11.0

**

.75

1.25

.625

.375

REFER
DRAWING #5
REVISED LOCATION

29/64 DRILL, TAP 1/2-20 UNF
14 HOLES

* FURTHER DETAIL - DRAWING NO. 1-A
** O-RING GROOVE FOR -267 RING

1.50

.50   .3125

7.875

2 REQUIRED

MOUNTING PLATE
FOR WINDOWS OF UMR SHOCK TUBE
SCALE: 3/8" = 1"   DRAWING NO. 1
                      DATE: 6-20-'67
JEW.

75.

BREAK CORNERS TO APPROX.
.005 RADIUS

0° TO 5°
TYP.

L

G
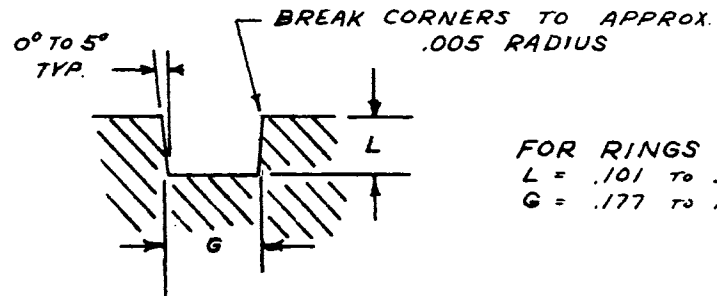
FOR RINGS NO.'S: 267, 263, 246
L = .101 TO .107
G = .177 TO .187

O-RING GROOVE DETAIL
SCALE: 3" = 1"

30°

8.00 DIA

.8890

7.115 DIA. (REF.)

7.875 DIA.

8.294 DIA.

O-RING #267

O-RING #263
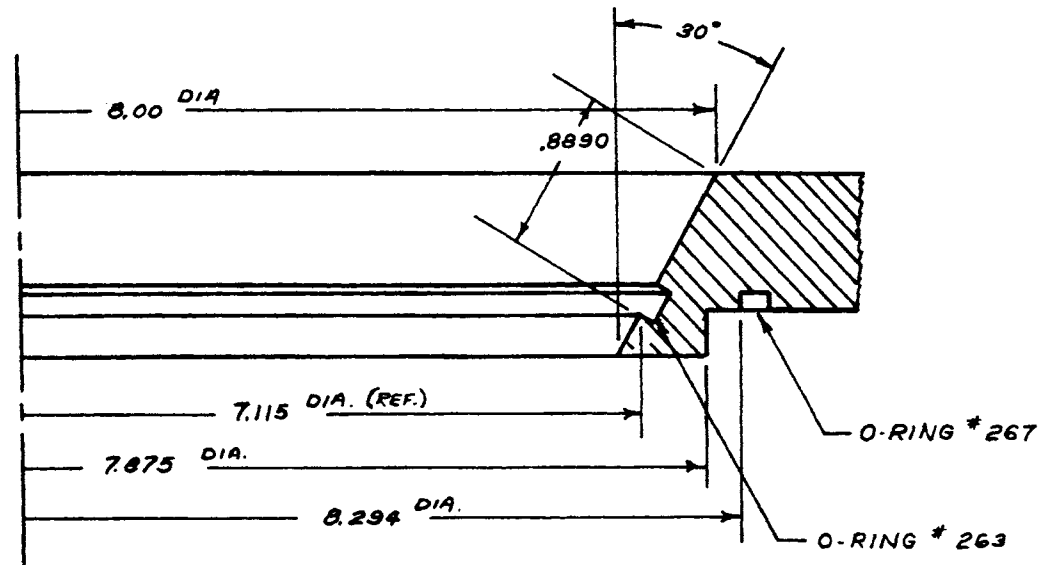
MOUNTING PLATE SEALS
FOR WINDOWS OF UMR SHOCK TUBE
SCALE: FULL   DRAWING NO. 1-A
J.E.W.   DATE: 7-10-67

76.

I DRILL $-\frac{3}{4}$ DEEP
$\frac{5}{16}$ -24 UNF TAP
$\frac{5}{8}$ DEEP
12 HOLES

1.00

30°

30°

8.00

.3125
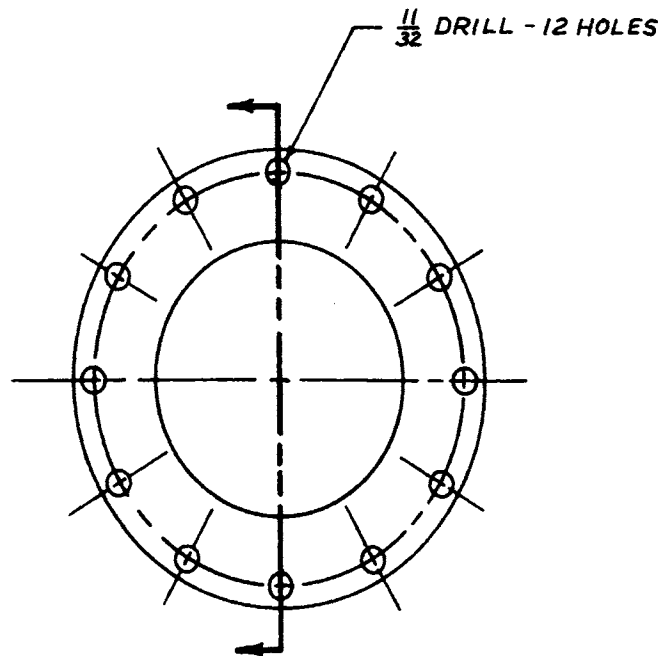
4.00

5.75

DETAIL ON DRAWING NO. 2-A
OF O-RING GROOVE -246 RING
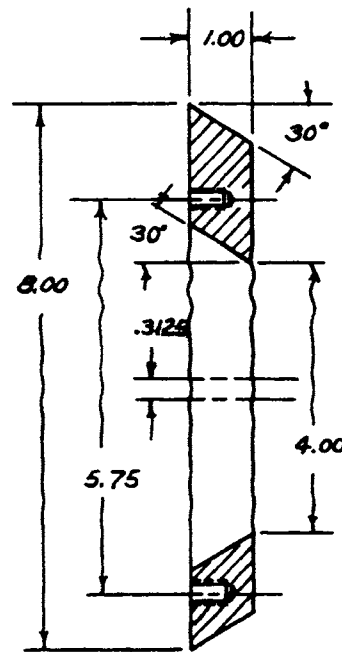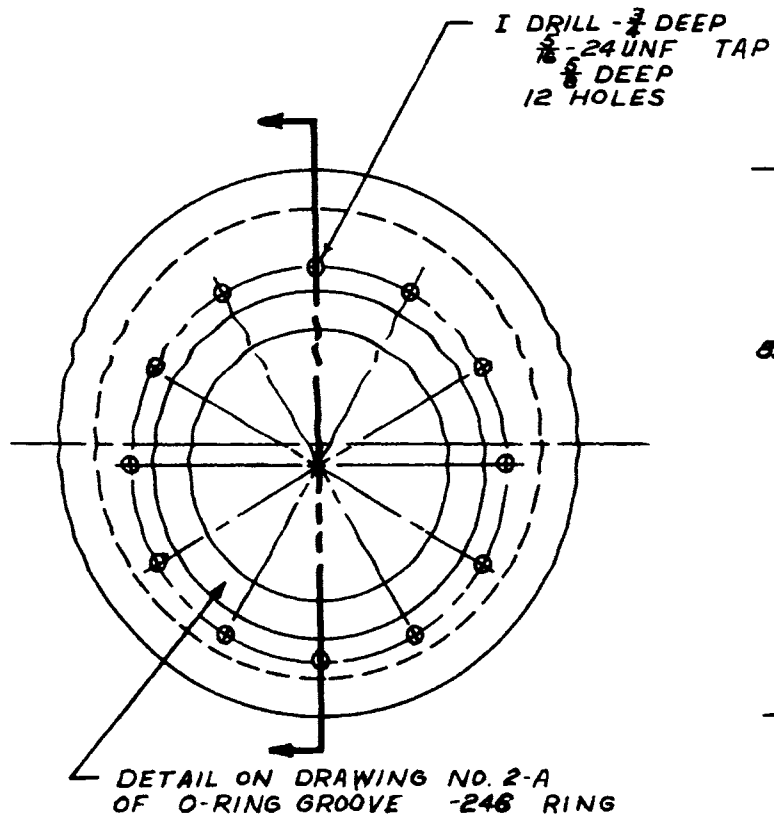
2 REQUIRED

SCHLIEREN WINDOW DISK
FOR WINDOWS OF UMR SHOCK TUBE
SCALE: $\frac{3}{8}$"= 1"   DRAWING NO. 2
J.E.W.   DATE: 6-20-'67

77.

30°
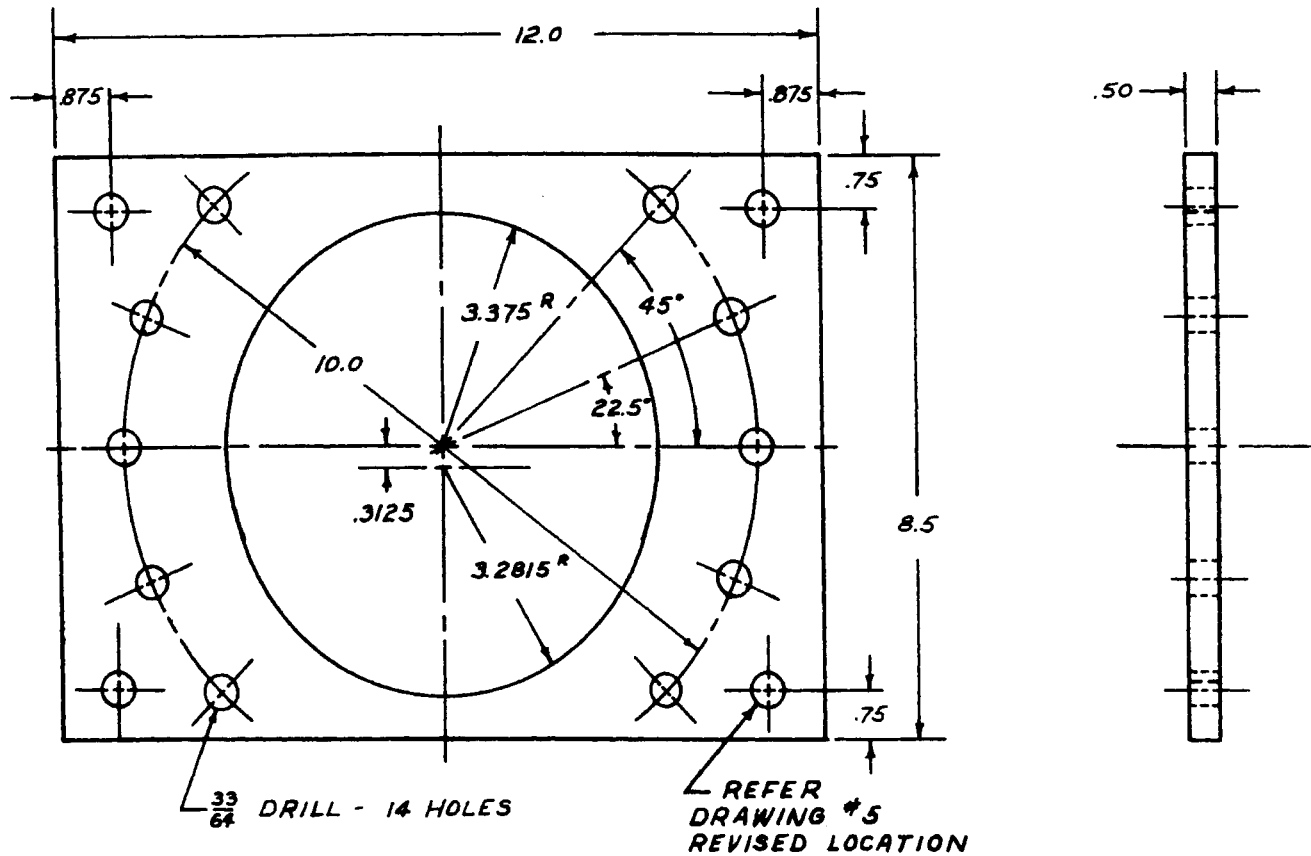
.364

4.00

4.364 DIA. (REF.)

O-RING # 246
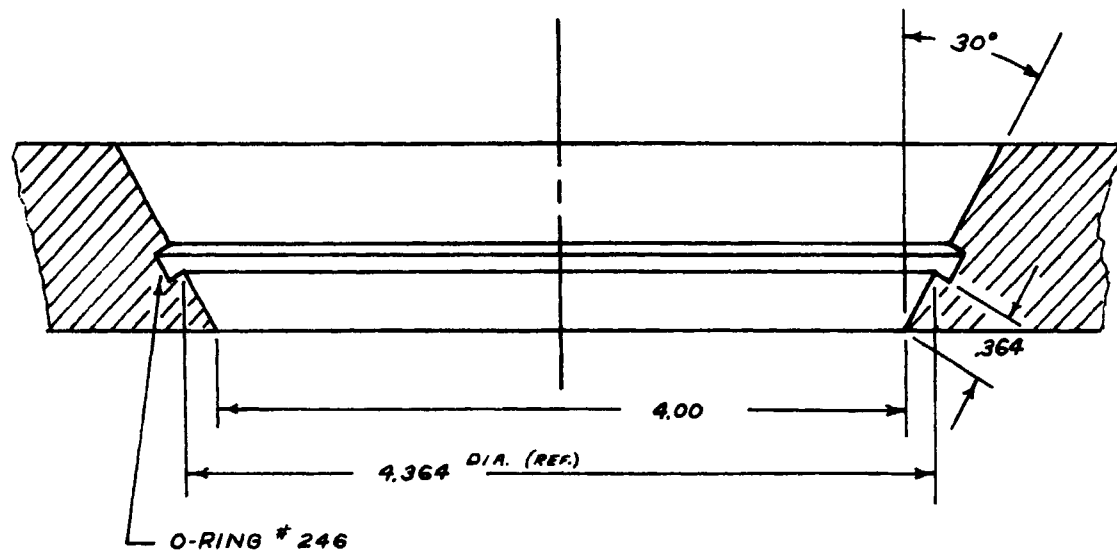
SCHLIEREN WINDOW SEAL
FOR WINDOWS OF UMR SHOCK TUBE
SCALE: FULL   DRAWING NO. 2-A
J.E.W.   DATE: 7-10-67

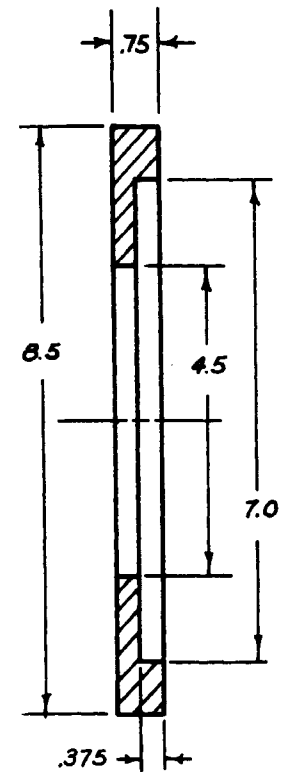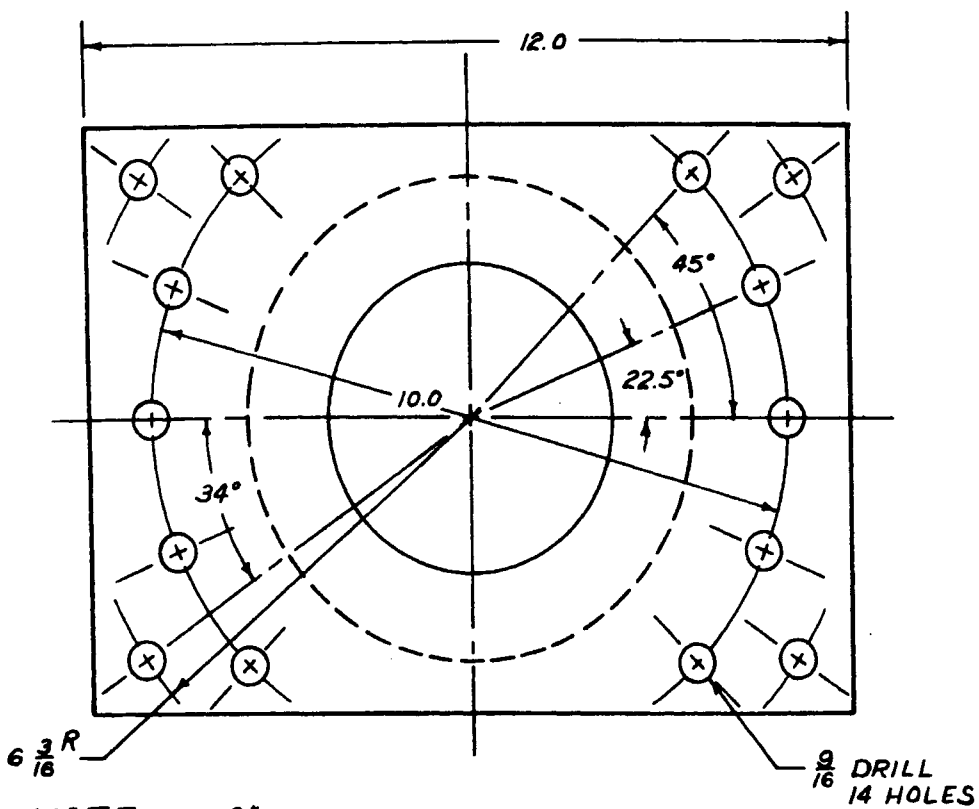$\frac{11}{32}$ DRILL - 12 HOLES

.50

5.75

3.875

6.40
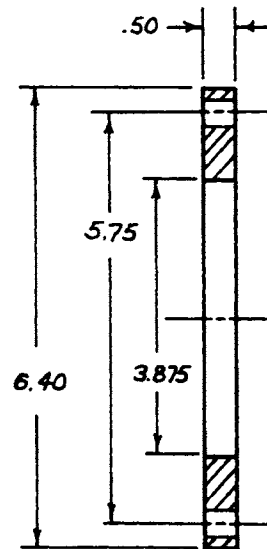
2 REQUIRED

"HOLD DOWN" RING

FOR WINDOWS OF UMR SHOCK TUBE

SCALE: $\frac{3}{8}" = 1"$ DRAWING NO. 3

J.E.W.   DATE: 6-20-67

12.0

.875 .875
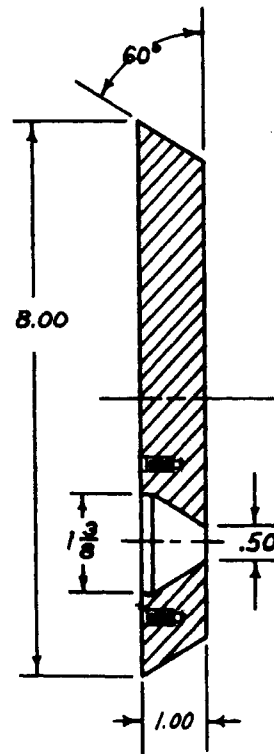
.75

3.375 R

45°

10.0

22.5°

.3125

8.5

3.2815 R

.50

33/64 DRILL - 14 HOLES

REFER
DRAWING #5
REVISED LOCATION

.75

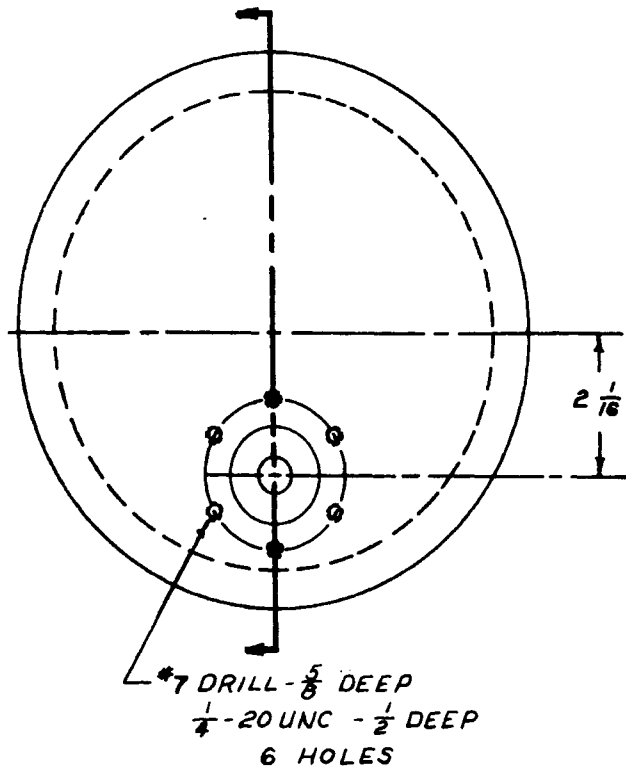COVER PLATE
FOR WINDOWS OF UMR SHOCK TUBE
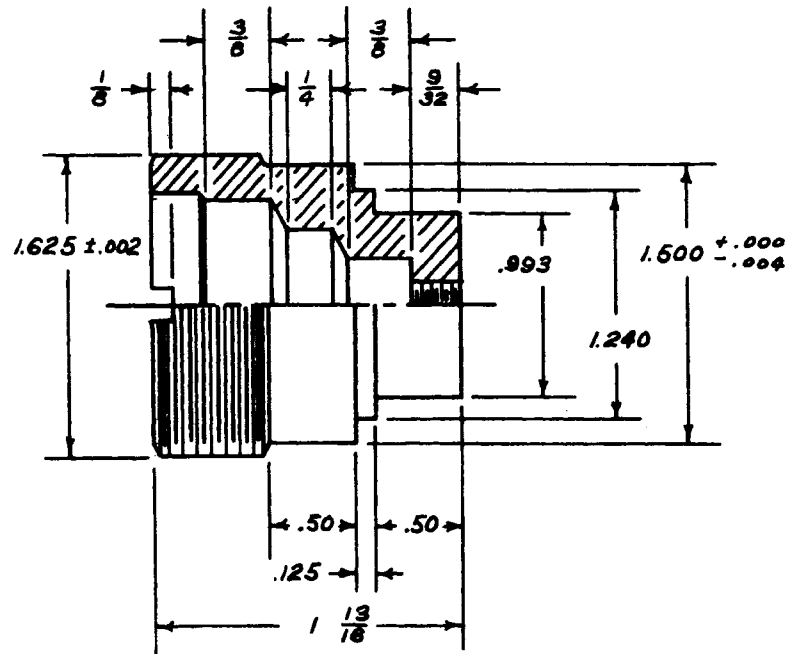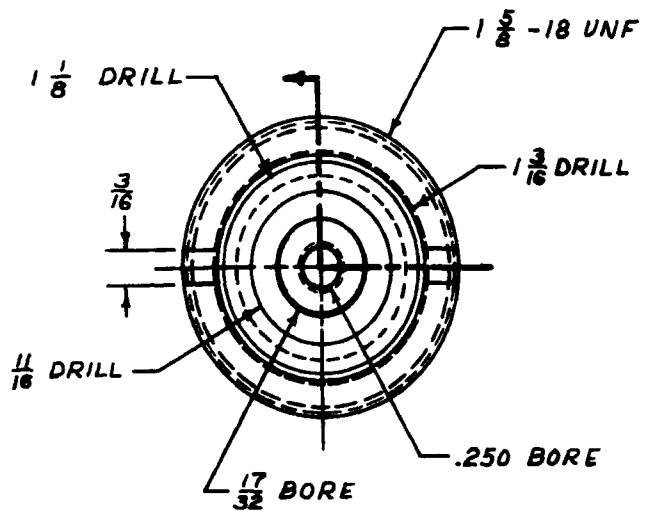SCALE: 3/8" = 1"   DRAWING NO. 4
        J.E.W.   DATE: 7-7-67

NOTE: $6\frac{3}{16}"$ - 34° LOCATION OF FOUR HOLES SUPERCEDES LOCATION DIMENSION ON DRAWINGS: 1 & 4

COVER PLATE REINFORCER WELDED TO COVER PLATE AT ENDS ONLY.

COVER PLATE REINFORCER
FOR WINDOWS OF UMR SHOCK TUBE
SCALE: $\frac{3}{8}" = 1"$ DRAWING NO. 5
J.E.W.   DATE: 9-28-'67

#7 DRILL - $\frac{5}{8}$ DEEP
$\frac{1}{4}$ - 20 UNC - $\frac{1}{2}$ DEEP
6 HOLES

2 $\frac{1}{16}$

60°

8.00

1 $\frac{3}{8}$

.50

1.00

INTERFEROMETER WINDOW DISK
FOR WINDOWS OF UMR SHOCK TUBE
SCALE: $\frac{3}{8}$" = 1"   DRAWING NO. 6
J.L.W.   DATE: 10-20-67

$1\frac{1}{8}$ DRILL

$1\frac{5}{8}$ -18 UNF

$1\frac{3}{16}$ DRILL

$\frac{3}{16}$

$\frac{11}{16}$ DRILL

.250 BORE

$\frac{17}{32}$ BORE

$\frac{3}{8}$

$\frac{3}{8}$

$\frac{1}{8}$

$\frac{1}{4}$

$\frac{9}{32}$

1.625 ± .002

.993

1.500 $+.000$ $-.004$

1.240

.50

.50

.125

$1\frac{13}{16}$

2 REQUIRED
MATERIAL: STAINLESS STEEL

TRANSDUCER ADAPTERS
FOR UMR SHOCK TUBE
SCALE: FULL   DRAWING NO. 7
J.C.W.   DATE: 10-20-67

83.

APPENDIX III

RELATION OF DENSITY GRADIENT TO THE

RADIUS OF CURVATURE OF A REFRACTED LIGHT RAY

The physical situation considered in this derivation is shown in Figure III-a. A wavefront of light which is perpendicular to the page passes through the test section of physical Length L. In the section, the light encounters gas of varying density such that the refractive index of part of the gas is n_1. At some differential distance Δs, the density has changed so that the refractive index is n_2. Assume that n_2 is greater than n_1 and that n_1 is very nearly unity, as is the case with gases.
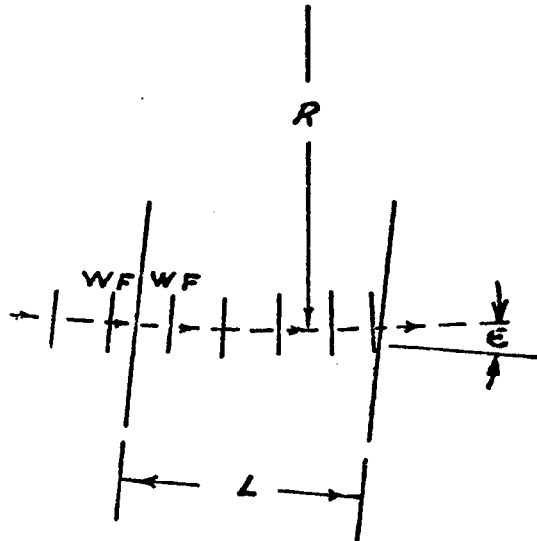

Figure III-a.   Wavefront Rotation

Since n_2 is greater than n_1, the light velocity in n_1 is greater than the light velocity in n_2 by virtue of Equation 2 on page 12.

Thus,

$$V_{n1} > V_{n2}$$
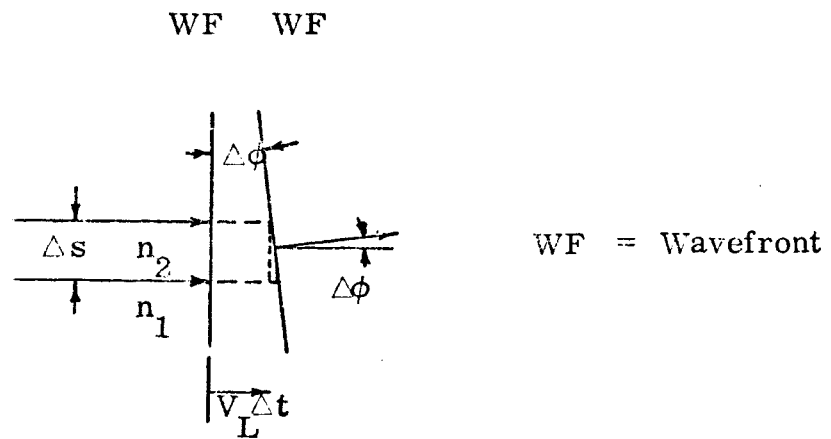
WF   WF

WF = Wavefront

Figure III-b.   Differential Rotation of Light Wavefront

The angle through which the wavefront rotates in time Δt is shown in Figure III-b and can be expressed as

$$\frac{(V_{n1} - V_{n2})\Delta t}{\Delta s} = \tan \Delta \phi \qquad \text{(III-1)}$$

Because $\Delta \phi$ is very small,

$$\tan \Delta \phi = \Delta \phi$$

The summation of the incremental rotations is the deflection angle ϵ, the total angular deflection of the light ray.

$$\sum_{0}^{T} \frac{(V_{n1} - V_{n2})\Delta t}{\Delta s} = \Sigma \Delta \phi = \epsilon \qquad \text{(III-2)}$$

but,

$$\frac{(V_{n1} - V_{n2})\Delta t}{\Delta s} = \frac{((V_{vac}/n_1) - (V_{vac}/n_2))\Delta t}{\Delta s}$$

thus

$$\sum_{0}^{T} \frac{V_{vac} \frac{n_2 - n_1}{n_2 n_1} \Delta t}{\Delta s} = \epsilon$$

$$\sum_{0}^{T} \frac{V_{vac}}{n_1 n_2} \frac{(n_2 - n_1)\Delta t}{\Delta s} = \epsilon \qquad (III-3)$$

Since n_1 is very nearly equal to unity,

$$\frac{V_{vac}}{n_1 n_2} = \frac{V_{vac}}{n_2} = V_{n2}$$

$$\sum_{0}^{T} V_{n2} \Delta t \frac{(n_2 - n_1)}{\Delta s} = \epsilon \qquad (III-4)$$

The summation of $(V_{n2}\Delta t)$ is equal to the test section length L if Δt is

the time necessary for the light traveling at velocity V_{n2} to travel the distance

L. Therefore,

$$L \frac{(n_2 - n_1)}{\Delta s} = \epsilon \qquad (III-5)$$

$$\lim_{\Delta s \to 0} L \frac{(n_2 - n_1)}{\Delta s} = L \frac{\partial n}{\partial s} = \epsilon \qquad (III-6)$$

The wavefront rotation causes the ray to follow a curved path through

the section and for small angles such as ϵ, the length of arc divided by the

radius of curvature is equal to the angle expressed in radians. Also for small

angles the arc length is very nearly equal to the tangent line, L in this case.

Therefore,

$$\frac{L}{R} = \epsilon \qquad\qquad\text{(III-7)}$$

But

$$L\frac{\partial n}{\partial s} = \epsilon \qquad\qquad\text{(III-6)}$$

and therefore,

$$\frac{\partial n}{\partial s} = \frac{1}{R} \qquad\qquad\text{(III-8)}$$

the density gradient equals the reciprocal of the radius of curvature of the

light ray.

VIII. VITA

The author, James Everett West, was born on January 24, 1944, in Edwardsville, Illinois. After graduation from Edwardsville High School he entered the University of Missouri at Rolla in September, 1962. A Bachelor of Science Degree in Mechanical Engineering was received from the University of Missouri at Rolla in August, 1966. At the same time, a commission as 2nd Lt. in the U. S. Army Reserve was received. In September, 1966, he entered the graduate school of the University of Missouri at Rolla to pursue studies toward a Master of Science Degree in Mechanical Engineering.